Different Reactive Oxygen Species Scavenging Properties of Flavonoids Determine Their Abilities to Extend the Shelf Life of Tomato[1][OPEN]

Yang Zhang[2], Rosalba De Stefano[2], Marie Robine[2], Eugenio Butelli, Katharina Bulling, Lionel Hill, Martin Rejzek, Cathie Martin*, and Henk-jan Schoonbeek

John Innes Centre, Norwich NR4 7UH, United Kingdom (Y.Z., R.D.S., M.Ro., E.B., K.B., L.H., M.Re., C.M., H.S.); and Department of Soil, Plant, Environmental, and Animal Sciences, University of Naples Federico II, 80138 Naples, Italy (R.D.S.)

ORCID IDs: 0000-0002-7793-1108 (Y.Z.); 0000-0002-6700-7587 (R.D.S.); 0000-0001-9147-9130 (L.H.); 0000-0002-3640-5080 (C.M.); 0000-0002-1087-2553 (H.S.).

The shelf life of tomato (*Solanum lycopersicum*) fruit is determined by the processes of overripening and susceptibility to pathogens. Postharvest shelf life is one of the most important traits for commercially grown tomatoes. We compared the shelf life of tomato fruit that accumulate different flavonoids and found that delayed overripening is associated with increased total antioxidant capacity caused by the accumulation of flavonoids in the fruit. However, reduced susceptibility to *Botrytis cinerea*, a major postharvest fungal pathogen of tomato, is conferred by specific flavonoids only. We demonstrate an association between flavonoid structure, selective scavenging ability for different free radicals, and reduced susceptibility to *B. cinerea*. Our study provides mechanistic insight into how flavonoids influence the shelf life, information that could be used to improve the shelf life of tomato and, potentially, other soft fruit.

Tomato (*Solanum lycopersicum*) is one of the most important agricultural products in the world as well as an important model for fleshy fruit ripening due to the tools and resources available for mechanistic investigations. Among the biggest challenges for the tomato industry is postharvest deterioration, which accounts for huge economic losses averaging over 25% of fresh produce every year. Different solutions have been employed to extend shelf life; the easiest and most widely used is to harvest fruit at the mature green stage and store them at low temperature. Subsequently, the fruit are exposed to ethylene to induce ripening. This can effectively reduce postharvest damage of the fruit during transportation. However, because fruit are ripened artificially, they lose much of their flavor and become tasteless (Maul et al., 1998, 2000). A large number of ripening-related mutants have also been used to extend shelf life (Kopeliovitch et al., 1979), including *ripening inhibitor, nonripening, never-ripe*, and *alcobaca* (Mutschler et al., 1992). Unfortunately, the inhibition of ripening in this way also results in an accompanying loss of flavor.

Shelf life of tomato is determined by two processes: the rate of fruit softening during overripening (which is the stage that follows commercial maturity, when the fruit softens and loses its organoleptic properties, including its characteristic taste and flavor), and susceptibility to opportunistic pathogens such as *Botrytis cinerea* (Cantu et al., 2009). *B. cinerea*, better known as gray mold, is the second most important fungal pathogen of plants, economically (Dean et al., 2012).

During the past 20 years, transgenic approaches have also been used to improve tomato shelf life. Most strategies to extend shelf life have focused on delaying overripening, including silencing several target genes such as those encoding cell well-degrading enzymes. Activation of cell well-degrading enzymes such as polygalacturonase and β-galactosidase at the climacteric is a major cause of fruit softening, and suppression of their expression has been used to delay fruit softening (Kramer et al., 1992; Meli et al., 2010). Another important group of

targets are encoded by ripening-related genes. By silencing inducers of ripening or overexpressing inhibitors of ripening, the shelf life of transgenic tomato fruit can be extended (Centeno et al., 2011).

The accumulation of reactive oxygen species (ROS) is associated with fruit ripening and overripening (Jimenez et al., 2002; Mondal et al., 2004). Postharvest application of antioxidant compounds can effectively extend tomato shelf life (Bhagwan et al., 2000), and extending shelf life by reducing ROS has also proved to be effective in other crops (Zidenga et al., 2012). A successful approach to extend shelf life has been to accumulate polyamines (PAs) in tomatoes. PAs have been found to decrease during fruit ripening, and increasing PA levels in fruit can enhance shelf life. This effect is associated with the high antioxidant capacity of PAs (Mehta et al., 2002; Nambeesan et al., 2010).

Due to their health benefits, there has been growing interest in the enrichment of flavonoids in crops (Muir et al., 2001; Winkel-Shirley, 2001; Bovy et al., 2002; Butelli et al., 2008; Luo et al., 2008; Zhang et al., 2014). The accumulation of anthocyanins in tomato fruit following fruit-specific expression of two transcription factors, Delila (Del) and Rosea1 (Ros1), from snapdragon (*Antirrhinum majus*) doubles shelf life (Zhang et al., 2013). Both the purple *Del/Ros1* tomato and the purple-skinned *Anthocyanin fruit* (*Aft*) and *atroviolacea* (*atv*; *Aft/Aft atv/atv*) tomato, produced by the introgression of *Solanum chilense* and *Solanum cheesmaniae* into tomato (Povero et al., 2011), show delayed overripening and reduced susceptibility to *B. cinerea* (Bassolino et al., 2013; Zhang et al., 2013). The accumulation of anthocyanins increases the total antioxidant capacity of tomatoes, slows the increase in ROS, and so delays overripening (Zhang et al., 2013). During infection of tomato fruit with necrotrophic pathogens such as *B. cinerea*, a burst of ROS generated by NADPH oxidases in both the host plant cells and in the fungal pathogen is induced by infection. The ROS burst is believed to contribute positively to the susceptibility of plants to *B. cinerea* (Govrin and Levine, 2000; Glazebrook, 2005). The high scavenging ability of anthocyanins may effectively alter ROS dynamics during *B. cinerea* infection and reduce the susceptibility of tomato fruit to this necrotrophic pathogen (Zhang et al., 2013).

High ROS-scavenging ability is a common feature of different flavonoids and has been attributed to the high reactivity of their hydroxyl groups to ROS (Heim et al., 2002). In vitro analysis indicates that the number of hydroxyl groups of flavonoids is important in determining the antioxidant capacity of flavonoids and their effectiveness in scavenging free radicals (Rice-Evans et al., 1996, 1997; Burda and Oleszek, 2001; Wang et al., 2006; Markovic et al., 2014). However, decoration (hydroxylation, methylation, glycosylation, and acylation) may affect the total antioxidant capacity of flavonoids and their ability to scavenge different free radical species (superoxide, hydroxyl radicals and ions, and hydrogen peroxide [H_2O_2]), and the specific scavenging abilities of decorated flavonoids cannot be predicted based solely on hydroxylation of the B-ring.

Tomato lines accumulating different flavonoid compounds have been produced (Butelli et al., 2008; Luo et al., 2008). As different flavonoid compounds have different antioxidant capacities and abilities to scavenge particular free radical species, tomato fruit accumulating different flavonoids may have different degrees of shelf life extension, as determined by both their rate of overripening and their susceptibility to *B. cinerea*.

To analyze the roles of different flavonoids in extending postharvest shelf life, orange flavonol-rich *AtMYB12* tomato fruit (Luo et al., 2008) were compared with red wild-type and *Del/Ros1* purple tomatoes using both storage and pathogen infection tests. To screen the activities of different flavonoids in determining tomato shelf life, virus-induced gene silencing (VIGS) was used to silence different biosynthetic genes to provide fruit tissues that accumulated different flavonoids and to test their impact on shelf life. Storage and pathogen tests were carried out in VIGS fruit and were confirmed using mutant lines. Our analyses showed that the structures of the accumulated flavonoids were linked through their abilities to scavenge total ROS to delay overripening and their abilities to scavenge specific ROS to reduce susceptibility to *B. cinerea*. Collectively, the effects on these two processes mean that specific flavonoids have differential effects on extending the shelf life of tomato. Our results have significance for breeding for extended shelf life in tomato and in many other fleshy fruit.

RESULTS

Lines of Tomato Used in Shelf-Life Studies

The purple *Del/Ros1* line N (*Del/Ros1* N) tomatoes have been described by Butelli et al. (2008) in terms of their metabolite composition and gene expression; similarly, the orange *AtMYB12* tomatoes have been described by Luo et al. (2008). A new line of tomato in the MicroTom genetic background was made by crossing *Del/Ros1* N MicroTom with *AtMYB12* MicroTom. The resulting line, named Indigo, contains high amounts of both anthocyanins and flavonols. The flavonoid contents of red wild-type, purple *Del/Ros1*, orange *AtMYB12*, and Indigo tomatoes in the MicroTom genetic background are shown in Supplemental Table S1. These values are in accordance with the values reported previously for the different genotypes in MicroTom and other genetic backgrounds (Butelli et al., 2008; Luo et al., 2008). The biosynthetic pathways for the production of flavonoids in tomato are shown in Figure 1.

Flavonol-Enriched Tomatoes Show Delayed Overripening

When stored in semisterile conditions, high-flavonol *AtMYB12* tomatoes showed delayed overripening compared with wild-type tomatoes. Fifty percent of wild-type fruit showed overripening symptoms after storage for 2 weeks at 17°C. For *AtMYB12* tomatoes, however,
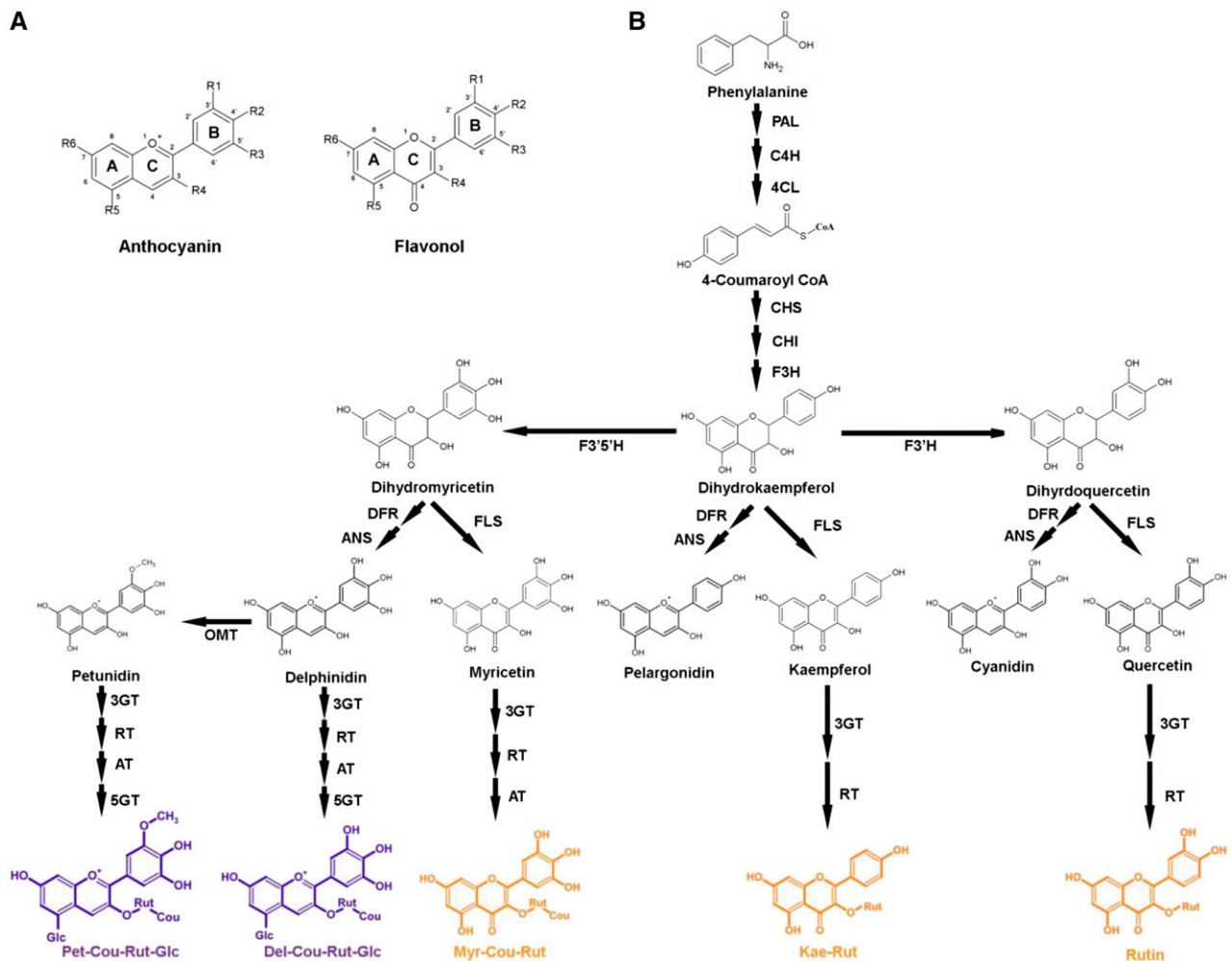
Figure 1. Flavonoid biosynthesis pathway in tomato. A, Basic structures of an anthocyanin and a flavonol. Common modification positions include 3′ (R1), 4′ (R2), 5′ (R3), 3 (R4), 5 (R5), and 7 (R6) of each ring. B, Schematic representation of the flavonoid biosynthetic pathway in tomato. Compounds highlighted in purple are the major anthocyanins identified in tomato fruit, and major flavonols are highlighted in orange. From the top, abbreviations are as follows: PAL, Phe ammonia lyase; 4CL, 4-coumarate: CoA ligase; C4H, cinnamate 4-hydroxylase; C3H, 4-coumarate 3-hydroxylase; CHS, chalcone synthase; CHI, chalcone isomerase; F3′H, flavonoid-3′-hydroxylase; FLS, flavonol synthase; DFR, dihydroflavonol reductase; ANS, anthocyanidin synthase; 3GT, flavonoid 3-O-glucosyltransferase; RT, flavonoid 3-O-glucoside-rhamnosyltransferase; AT, anthocyanin acyltransferase; 5GT, flavonoid-5-glucosyltransferase; and OMT, O-methyltransferase.

the date for a similar level of overripening was delayed to 3 to 4 weeks after the start of storage. For *Del/Ros1* and Indigo tomatoes, longer storage times (5–6 weeks) were needed to see the same degree of overripening (Fig. 2A). The fresh weight of the four lines showed the same rate of reduction over the first 4 weeks of storage. However, beyond 4 weeks, the rate of reduction in fresh weight of *AtMYB12* tomatoes increased significantly, whereas other lines maintained the same rate of reduction (Fig. 2B).

The delayed overripening of *AtMYB12* tomatoes compared with the wild type was also observed in fruit left on the vine. Overripening could be seen on wild-type fruit from 4 weeks after breaker. For *AtMYB12* tomatoes, however, 6 to 8 weeks after breaker were needed to observe the same degree of overripening. After 8 weeks, *AtMYB12* fruit overripened very rapidly.

For purple *Del/Ros1* and Indigo tomatoes, a similar degree of overripening was seen only at 8 to 10 weeks after breaker (Supplemental Fig. S1).

Collectively, these data indicate that, compared with wild-type tomatoes, high-flavonol *AtMYB12* tomatoes show delayed overripening. However, the length of the delay was not as great as for purple *Del/Ros1* or Indigo (*Del/Ros1;AtMYB12*) tomatoes.

The Antioxidants in Orange *AtMYB12* Fruit Are Less Stable Than Those in Purple *Del/Ros1* Tomatoes

The high antioxidant capacity of anthocyanin-enriched tomatoes reduces oxidative damage to fruit tissues and, consequently, delays overripening (Bassolino et al., 2013;
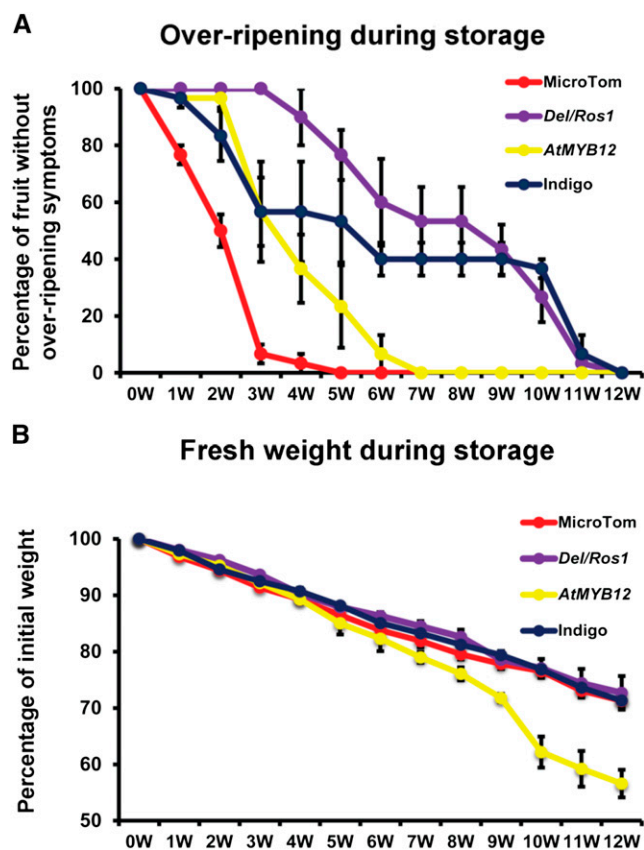
A

Over-ripening during storage

B

Fresh weight during storage

Figure 2. *AtMYB12* tomatoes store for longer than wild-type MicroTom but for less time than *Del/Ros1* and Indigo tomatoes. Fruit were harvested at 14 d post breaker (0W). A, The percentages of fruit showing the symptoms of overripening were assessed every week during storage tests. B, Fresh weights of different fruit during storage. The total weight of the 10 fruit in the same jar was calculated. Error bars show SE (*n* = 3).

Zhang et al., 2013). We checked the total hydrophilic antioxidant capacities of the four lines used in the storage tests at different stages of overripening using the trolox equivalent antioxidant capacity (TEAC) assay, which is recommended for measuring the total antioxidant capacity of polyphenols (Rice-Evans et al., 1997). For all the transgenic lines (high anthocyanin [*Del/Ros1*], high flavonol [*AtMYB12*], and high anthocyanin/high flavonol [Indigo]), the antioxidant capacity of hydrophilic compounds was found to increase significantly at breaker compared with wild-type tomatoes (Supplemental Fig. S2A). This was due to the induction of flavonoid biosynthesis by the E8 promoter, which was used to drive the expression of the different transcription factors from breaker onward. Breaker is the point at which ethylene starts to rise in tomato fruit and is marked by the onset of lycopene biosynthesis and the change in fruit color. The expression of Del, Ros1, and AtMYB12 transcription factors enhanced the production of different flavonoids, which increased the antioxidant capacities of the mature fruit.

During overripening, the total antioxidant capacity of *AtMYB12* tomatoes showed more rapid decline than in *Del/Ros1* and Indigo tomatoes: significant reductions

in the antioxidant capacity of *AtMYB12* fruit came 8 weeks after breaker. However, for *Del/Ros1* and Indigo tomatoes, significant reductions in antioxidant capacity were not seen until 10 weeks after breaker (Supplemental Fig. S2A). The lower stability of the elevated antioxidant capacity of *AtMYB12* tomatoes was associated with the more rapid decline in fresh weight of these tomatoes late in the storage tests (Fig. 2B). This suggested that the flavonoids contributing to antioxidant capacity in *AtMYB12* tomatoes were less stable than those in *Del/Ros1* and Indigo tomatoes.

To test this hypothesis, production of malondialdehyde (MDA), a by-product of lipid peroxidation that can be used as a marker for the damage resulting from ROS during senescence (Dhindsa et al., 1981; Zhang et al., 2013), was measured for all the tomato lines. For wild-type MicroTom fruit, MDA production increased throughout the entire late ripening period. However, for all the transgenic lines, the MDA levels remained low up to 4 weeks after breaker. For the *AtMYB12* line, the MDA levels increased at 6 weeks after breaker, when the total antioxidant capacity of *AtMYB12* tomatoes began to decrease significantly. For *Del/Ros1* tomatoes, the increase in MDA levels came 8 weeks after breaker (Supplemental Fig. S2B). This matched the delayed reduction of antioxidant capacity in *Del/Ros1* fruit.

Accumulation of Different Flavonoids in Tomato Fruit Using VIGS

To analyze in more detail which flavonoids contribute directly to extending shelf life, three anthocyanin biosynthetic genes (Fig. 1; *FLAVANONE 3-HYDROXYLASE* [*SlF3H*], *DIHYDROFLAVONOL 4-REDUCTASE* [*SlDFR*], and *ANTHOCYANIDIN SYNTHASE* [*SlANS*] from tomato) were silenced separately in purple tomatoes using VIGS (Orzaez et al., 2009). VIGS works well in globe tomatoes, so purple Del/Ros1 tomatoes in the MoneyMaker genetic background were used (Orzaez et al., 2009; Zhang et al., 2013). Silencing of *SlF3H*, *SlDFR*, and *SlANS* by VIGS effectively blocked the production of anthocyanins in *Del/Ros1* MoneyMaker fruit. The silenced sectors accumulated far fewer anthocyanins (Fig. 1; Supplemental Fig. S3A). Reverse transcription (RT)-quantitative PCR (qPCR) of complementary DNA from both nonsilenced and silenced sectors on the same fruit indicated that the silencing of anthocyanin biosynthetic genes did not affect the expression of *Del/Ros1*. However, when *SlF3H* was silenced, the expression of biosynthesis genes early in the pathway (*PHENYLALANINE AMMONIA LYASE*, *CHALCONE SYNTHASE*, and *CHALCONE ISOMERASE*) as well as *SlDFR* was reduced (Supplemental Fig. S3B). When *SlDFR* was silenced, there was no significant reduction in the expression levels of any other genes (Supplemental Fig. S3B). In VIGS-*SlANS*-silenced sectors, although late anthocyanin biosynthetic genes (*SlF3H*, *SlDFR*, and *SlANS*) were silenced, there was a substantial induction of *FLAVONOID 3'5' HYDROXYLASE* (*SlF3'5'H*) expression (Supplemental Fig. S3B).

F3′5′H is a P450 enzyme that catalyzes the addition of –OH groups to the C-3′ and 5′ positions on the B-ring of flavonoids (Holton et al., 1993; Olsen et al., 2009). When *F3′5′H* expression was induced, flavonoids with three –OH groups on the B-ring were produced. Liquid chromatography-mass spectrometry (LC-MS) data indicated that very little anthocyanin was present in any of the silenced sectors of VIGS-*SlF3H*, VIGS-*SlDFR*, and VIGS-*SlANS* fruit (Supplemental Figs. S4A and S5). However, the VIGS-*SlANS*-silenced sectors contained increased amounts of myricetin (a flavonol that has three –OH groups on its B-ring; Fig. 1) derivatives (compound 8; Supplemental Figs. S4B and S5B), which result from the induction of *F3′5′H* expression.

The Shelf Life of VIGS Fruit Is Positively Correlated with the Total Antioxidant Capacity of the Silenced Sectors

The total antioxidant capacity of silenced sectors on different VIGS fruit was different because these sectors accumulated different flavonoids. Compared with wild-type MoneyMaker fruit, the antioxidant capacity of hydrophilic compounds was about 3-fold higher in *Del/Ros1* MoneyMaker fruit. However, in silenced sectors of different VIGS fruit, the total antioxidant capacities were decreased. Silencing of *Del* and *Ros1* in purple tomato removed most of the increase in antioxidant capacity, and VIGS-*Del/Ros1* fruit had only marginally higher TEAC values than wild-type fruit. Silencing of *SlF3H* and *SlDFR* resulted in the absence of most of the anthocyanins (present in the purple, nonsilenced sectors), and the TEAC values of the silenced sectors were only 2-fold higher than those of wild type tomatoes. For VIGS-*SlANS* fruit, although silenced sectors did not have most of the anthocyanins that were present in purple sectors, enrichment in myricetin derivatives compensated in part, and the silenced VIGS-*SlANS* sectors had TEAC values 2.5-fold higher than those of wild-type fruit (Fig. 3A).

Storage tests of ripe fruit showed a good correlation between total antioxidant capacity and storage time. VIGS-*SlF3H* fruit showed ripening defects (the silenced parts showed uneven ripening and the fruit tissues became very hard). Compared with wild-type fruit, VIGS-*SlF3H*, VIGS-*SlANS*, and *Del/Ros1* fruit showed significant delays in overripening (Fig. 3B). However, for VIGS-*SlDFR* fruit sectors, as their antioxidant capacity was significantly lower than that of untreated *Del/Ros1* fruit tissue, their viable storage period was significantly shorter than that for *Del/Ros1* fruit (Fig. 3B). These data confirmed that increased total antioxidant capacity is the main cause of the delay in overripening in purple tomatoes.

Natural Mutants Confirm the Importance of Total Antioxidant Activity to the Length of the Overripening Period

To confirm the results of VIGS on overripening in VIGS-*SlDFR* and VIGS-*SlANS* fruit, two anthocyanin mutants in the Ailsa Craig genetic background, *aw*
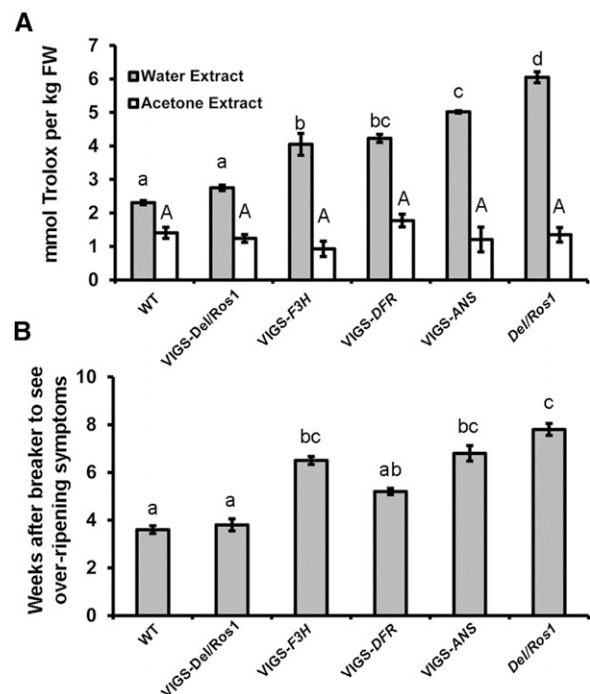

Figure 3. Silencing of different anthocyanin biosynthetic genes in *Del/Ros1* tomatoes by VIGS showed different effects on fruit storage time. A, Total antioxidant capacity of water and acetone extracts from wild-type (WT) and different VIGS fruit. Fruit were harvested at 14 d post breaker. Error bars show SE ($n = 3$). Different letters indicate significantly different values at $P < 0.05$ (one-way ANOVA, Tukey's posthoc test) using the same extraction method. FW, Fresh weight. B, Times of storage needed to see overripening symptoms in different VIGS fruit. Fruit were harvested 2 weeks after breaker, and the time to show overripening symptoms (visual rotting and collapse of fruit) was recorded. Error bars show SE ($n = 10$). Different letters indicate significantly different values at $P < 0.05$ (multiple pairwise comparison using χ^2 test).

(LA3281) and *ae* (LA3612), were crossed with the *Del/Ros1* tomato line, and $aw^{-/-}$ *Del/Ros1* and $ae^{-/-}$ *Del/Ros1* lines were selected in the F2 generation. The *aw* mutant is DFR deficient, and *ae* lacks ANS activity (Goldsbrough et al., 1994; De Jong et al., 2004).

Compared with *Del/Ros1* Ailsa Craig fruit, $aw^{-/-}$ *Del/Ros1* fruit produced no anthocyanins but were enriched in kaempferol derivatives (Fig. 4A; Supplemental Fig. S6). The hydrophilic antioxidant capacity was 2-fold higher than that of wild-type Ailsa Craig fruit (Fig. 4B). No anthocyanins accumulated in $ae^{-/-}$ *Del/Ros1* fruit either, but the content of myricetin derivatives increased (Fig. 4A; Supplemental Fig. S6), confirming the result of *ANS* silencing in VIGS fruit. The TEAC value of $ae^{-/-}$ *Del/Ros1* fruit was about 3-fold that of the wild type (Fig. 4B).

Storage tests showed similar results to the VIGS fruit storage tests. On average, $aw^{-/-}$ *Del/Ros1* fruit stored for longer, although the difference was not significant compared with wild-type fruit (Fig. 4C). Compared with wild-type fruit, $ae^{-/-}$ *Del/Ros1* fruit had a significantly longer shelf life. These results matched the TEAC values of these lines (Fig. 4B). Together, these data

support the conclusion that the degree of delay in overripening is dependent on the total antioxidant capacity of the tomato fruit (Fig. 5).

AtMYB12 Tomatoes Are Susceptible to the Fungal Pathogen *B. cinerea*

We extended our analysis to investigate the second facet of postharvest shelf life by examining the effects of different flavonoids on the susceptibility of fruit to the necrotrophic pathogen *B. cinerea*. Anthocyanin-enriched *Del/Ros1* tomatoes show low susceptibility to *B. cinerea*,
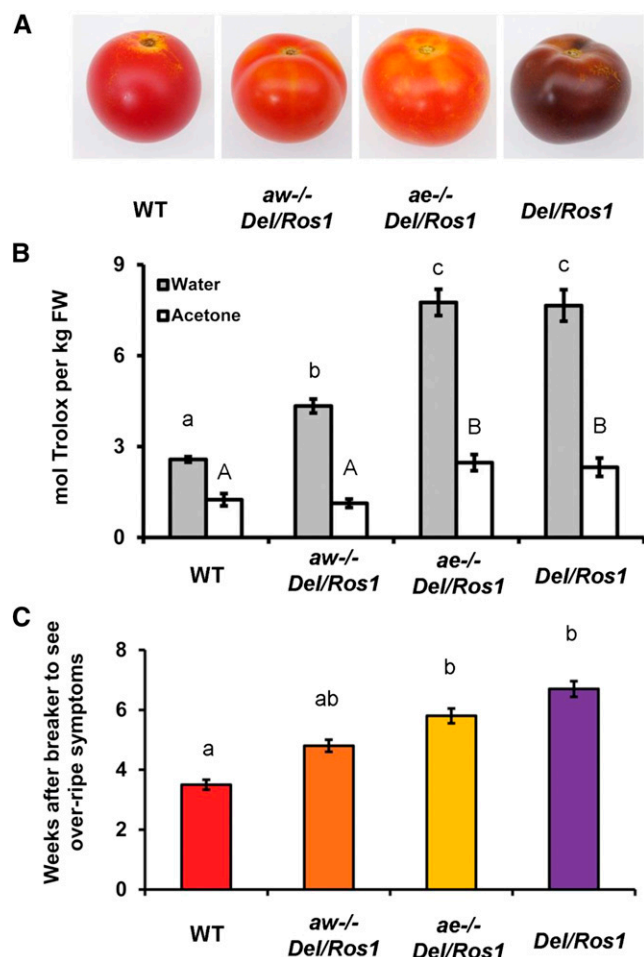

Figure 4. Blocking anthocyanin accumulation using different mutants affecting anthocyanin biosynthetic genes showed different effects on fruit shelf life. A, Phenotypes of *Del/Ros1* tomato crossed with anthocyanin biosynthetic mutants. B, Antioxidant capacity of different fruit. Fruit were harvested at 14 d post breaker. Error bars show SE (*n* = 3). Different letters indicate significantly different values at *P* < 0.05 (one way ANOVA, Tukey's posthoc test) using the same extraction method. FW, Fresh weight. C, Storage tests of different fruit. Fruit were harvested 2 weeks after breaker, and the times needed to show overripening symptoms (visual rotting and collapse of fruit) were recorded. Error bars show SE (*n* = 10). Different letters indicate significantly different values at *P* < 0.05 (multiple pairwise comparison using χ^2 test). WT, Wild type.

one of the most important postharvest pathogens of tomato fruit (Bassolino et al., 2013; Zhang et al., 2013). To investigate the susceptibility of high-flavonol *AtMYB12* tomatoes to the pathogen, both wound-inoculated and spray-infected fruit were tested for susceptibility to *B. cinerea*.

When intact fruit were sprayed with *B. cinerea* spores, the percentage of fruit showing severe symptoms was high for both wild-type and *AtMYB12* tomatoes at 5 d post inoculation (dpi). However, very few of the purple *Del/Ros1* or Indigo fruit showed severe infection (Fig. 6A). χ^2 analysis indicated that the distribution of different resistance patterns was similar in *AtMYB12* and wild-type fruit, which were significantly different from *Del/Ros1* and Indigo tomatoes. This suggested that *AtMYB12* fruit are as susceptible as wild-type fruit to *B. cinerea* infection by spraying.

Fruit were also wound inoculated with *B. cinerea* spores. At 1 dpi, the size of the lesions was the same in all fruit types. From 2 dpi, however, there was greater spread of infection in wild-type and *AtMYB12* fruit than in *Del/Ros1* and Indigo fruit. At 3 dpi, the average size of the lesions in wild-type and *AtMYB12* tomatoes was significantly larger than in *Del/Ros1* and Indigo fruit, indicating that they were more susceptible to *B. cinerea* infection (Fig. 6B). qPCR with DNA extracted from infected tomatoes confirmed that there was significantly more *B. cinerea* growing on wild-type and *AtMYB12* fruit than on *Del/Ros1* and Indigo fruit at 3 dpi (Fig. 6C).

The susceptibility of tomato fruit to necrotrophic pathogens increases as ripening progresses (Cantu et al., 2008, 2009). When fruit at different stages were infected by *B. cinerea*, a correlation between ripening and increased susceptibility was seen in both wild-type and *AtMYB12* lines. However, in *Del/Ros1* and Indigo lines, there was no significant increase in susceptibility to *B. cinerea* after breaker (Fig. 6D).

AtMYB12 was also expressed in globe MoneyMaker fruit (Luo et al., 2008). *AtMYB12* MoneyMaker fruit were very susceptible to infection by *B. cinerea* (Supplemental Fig. S7). Collectively, these data suggested that, unlike *Del/Ros1* tomatoes, high-flavonol *AtMYB12* tomatoes are as susceptible as wild-type tomatoes to postharvest infection by *B. cinerea*.

AtMYB12 Tomatoes Do Not Show Alterations in the Dynamics of the ROS Burst during *B. cinerea* Infection

To investigate the high susceptibility of *AtMYB12* tomatoes to *B. cinerea* infection, RT-qPCR was undertaken to check the expression of important pathogen response genes before and after inoculation. The expression of major pathogen response genes (*CHITINASE*, *β-1,3-GLUCANASE*, *METACASPASE7*, *PATHOGENESIS-RELATED PROTEIN1*, and *HYPERSENSITIVITY-RELATED GENE203* [*SlHSR203*]) was induced in both wild-type and *AtMYB12* tomatoes following inoculation as well as in *Del/Ros1* purple tomatoes (Supplemental
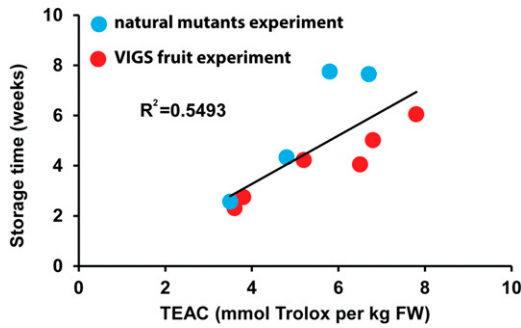
Figure 5. Relationship between total hydrophilic antioxidant capacity and the shelf life of tomato fruit. Data from Figures 3 and 4, B and C, were combined to compare the antioxidant capacity of fruit with their shelf life. FW, Fresh weight.

Fig. S8, A–D). This indicated that normal defense responses were operational in all the lines. However, a hypersensitive response (HR) gene, *SlHSR203*, was highly expressed in wild-type and *AtMYB12* tomatoes following inoculation, while in *Del/Ros1* tomatoes, induction of *SlHSR203* was much lower (Supplemental Fig. S8E). *HSR203* expression is associated with HR-triggered cell death (Pontier et al., 1998; Tronchet et al., 2001). These data suggested that the HR in *AtMYB12* tomatoes is very strong following infection with *B. cinerea*.

The total antioxidant capacities of both infected and wound-only fruit were measured. After *B. cinerea* infection, the total antioxidant capacity of wild-type and *AtMYB12* fruit declined compared with fruit without infection. For *Del/Ros1* tomatoes, however, the total antioxidant capacity was stable following inoculation with *B. cinerea* (Supplemental Fig. S8F).

Anthocyanins alter the dynamics of the ROS burst during the *B. cinerea* infection of tomato fruit, restricting the spread of H_2O_2 around the infection site and limiting the area of dead and dying cells, thus altering the susceptibility to infection (Zhang et al., 2013). In order to check the influence of flavonols on ROS dynamics and pathogen susceptibility, 3,3'-diaminobenzidine staining for H_2O_2 in fruit was undertaken between 24 and 48 h after *B. cinerea* infection. For wild-type and AtMYB12 tomatoes, the ROS burst spread widely around the infection site. However, for *Del/Ros1* and Indigo tomatoes, the ROS burst was restricted to the initial inoculation sites (Fig. 7A). Although high-flavonol *AtMYB12* fruit have high total antioxidant capacity compared with wild-type fruit before pathogen infection and a total antioxidant capacity equivalent to that of *Del/Ros1* purple fruit (Fig. 8A; Supplemental Fig. S8F), they have reduced/no ability to alter the dynamics of the ROS burst during *B. cinerea* infection compared with high-anthocyanin *Del/Ros1* tomatoes. These data showed that although anthocyanin-enriched tomato fruit have altered ROS
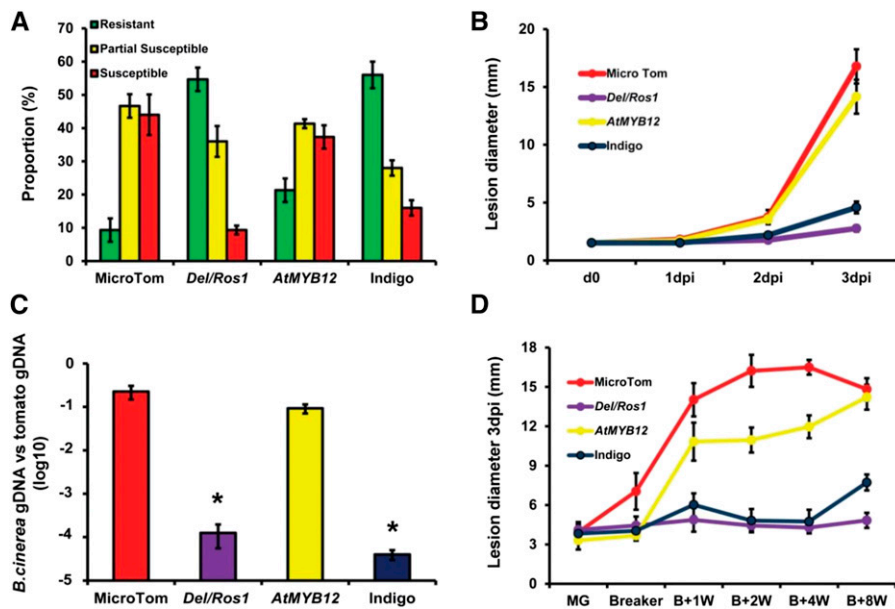

Figure 6. *AtMYB12* tomatoes are susceptible to *B. cinerea*. A, Different degrees of susceptibility to *B. cinerea* were shown by wild-type, *AtMYB12*, *Del/Ros1*, and Indigo fruit in spraying tests. Fruit were inspected at 5 dpi. Error bars represent sᴇ for three independent assays. Green bars show the percentage of resistant fruit, yellow bars show partially susceptible fruit, and red bars show susceptible fruit. B, Lesion development on wounded fruit infected with *B. cinerea*. Error bars represent sᴇ ($n = 6$). C, qPCR estimating the amount of *B. cinerea* growing on wounded, infected fruit at 3 dpi. *B. cinerea* growth was calculated by comparison of the ratio of *B. cinerea* DNA to tomato DNA. Error bars show sᴇ ($n = 3$). Asterisks indicate significant differences ($P < 0.05$) compared with MicroTom. gDNA, Genomic DNA. D, Ripening-related susceptibility of tomatoes enriched with different flavonoids to *B. cinerea*. Fruit of different flavonoids were harvested at different time points and inoculated with *B. cinerea* spores. Lesion sizes were measured at 3 dpi. Error bars represent sᴇ for three independent assays.

burst dynamics during *B. cinerea* infection, flavonol-enriched (rutin and kaempferol 3-*O*-rutinoside [Kae-Rut]) tomatoes do not have altered ROS burst dynamics and are effectively as susceptible to *B. cinerea* infection as wild-type fruit.

To confirm the role of ROS dynamics on pathogen susceptibility, fruit from the different lines were pretreated with diphenyleneiodonium chloride (a ROS inhibitor) and Glc oxidase plus Glc (a ROS inducer; Govrin and Levine, 2000; Zhang et al., 2013). Compared with water-treated fruit, diphenyleneiodonium chloride-treated wild-type and *AtMYB12* fruit had smaller lesion sizes at 3 dpi. For *Del/Ros1* and Indigo tomatoes, Glc oxidase plus Glc treatment increased their susceptibility to *B. cinerea* (Fig. 7B). These data confirmed that the ROS burst contributes positively to the susceptibility to *B. cinerea* infection and that *AtMYB12* tomatoes have an appreciably lower ability to alter ROS dynamics than *Del/Ros1* purple tomatoes during pathogen infection.

Different Flavonoids Contribute Specifically to the Lower Susceptibility of *Del/Ros1* Tomatoes to *B. cinerea*

Although purple tomatoes showed significantly lower susceptibility to *B. cinerea*, supplementation of agar with *Del/Ros1* tomato juice did not inhibit the growth of *B. cinerea* on plates (Zhang et al., 2013). The total antioxidant capacity of *AtMYB12* tomato juice was as high as that of juice from the *Del/Ros1* and Indigo lines (Fig. 8A), yet the different flavonoid-enriched tomato lines showed

different susceptibilities to *B. cinerea*. To test the effects of different flavonoids on *B. cinerea* infection in fruit, we developed an assay using extracts from fruit in combination with *B. cinerea* inoculation. Fruit juices (from wild-type, *AtMYB12*, *Del/Ros1*, and Indigo tomatoes) were added to *B. cinerea* inocula of wild-type fruit. The addition of juice from wild-type MoneyMaker, wild-type MicroTom, and *AtMYB12* tomatoes did not reduce lesion development significantly compared with water control supplements following inoculation with *B. cinerea* spores (Fig. 8B). However, juice from the *Del/Ros1* and Indigo lines effectively reduced the susceptibility of fruit when supplied together with *B. cinerea* spores in inoculations (Fig. 8B). Although all the transgenic lines had higher total antioxidant capacities than the wild-type line, supplementation of juices from these lines with *B. cinerea* inocula had differential effects. We concluded that specific compounds, present in *Del/Ros1* (and Indigo) tomatoes only, contributed to the reduced susceptibility to *B. cinerea* of these lines.

Susceptibility of VIGS Fruit to *B. cinerea* Infection

To identify which flavonoids in tomato affected the susceptibility of fruit to *B. cinerea*, we investigated the infection of silenced sectors of VIGS-*F3H*, VIGS-*DFR*, and VIGS-*ANS* fruit. When the silenced sectors of different VIGS fruit were inoculated with *B. cinerea* and compared with *Del/Ros1* tomatoes at 3 dpi, *SlANS*-silenced fruit showed nearly the same level of resistance
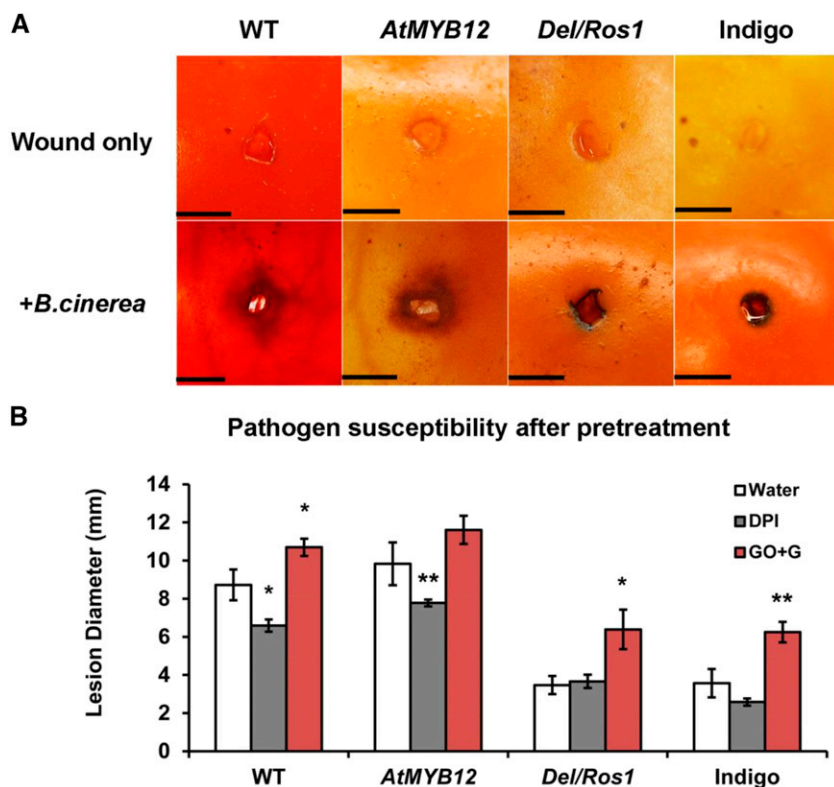
Figure 7. ROS contributes positively to the susceptibility to *B. cinerea* of tomato fruit. A, Wild-type (WT) and *AtMYB12* tomato fruit have lower ability to restrict the ROS burst compared with *Del/Ros1* and Indigo tomatoes. 3,3'-Diaminobenzidine staining of H_2O_2 is shown between 24 and 36 h after inoculation of *B. cinerea* on different lines. Wound-only fruit were used as controls. Bars = 1 mm. B, *B. cinerea* infection of pretreated fruit. Fruit were pretreated with water, 50 μM diphenyleneiodonium chloride (DPI), and 100 units mL^{-1} Glc oxidase + 1% Glc (GO+G) before *B. cinerea* infection. Lesion diameter was measured at 3 dpi. Error bars show SE (n = 10). *, $P < 0.05$; and **, $P < 0.01$ indicate significant differences compared with the water treatment of the same genotype.

Figure 8. Tomato juices enriched with different flavonoids have different effects on *B. cinerea* infection of tomatoes. A, Total antio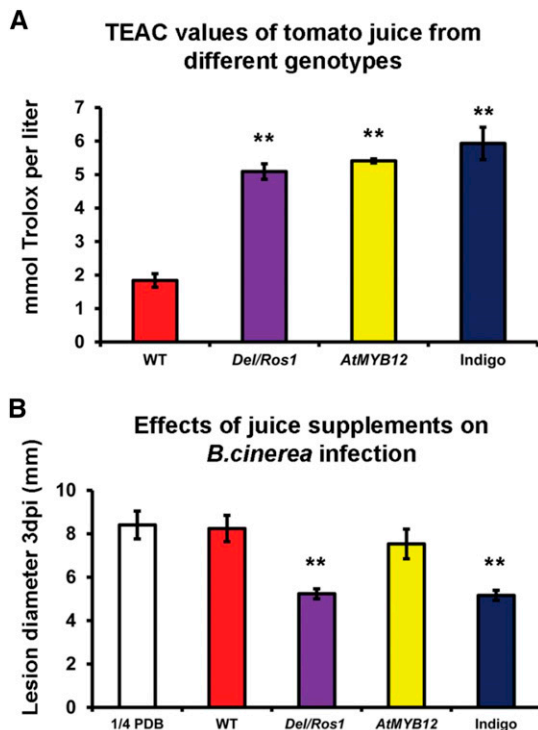xidant capacity of different tomato juices. Error bars show SE ($n = 3$). **, $P < 0.01$ compared with wild-type (WT) juice. B, Juice supplements to *B. cinerea* inoculum on wild-type MoneyMaker fruit differentially affect susceptibility. Different juices were supplied to different inoculation sites on wild-type fruit, and lesion sizes at 3 dpi were measured. Error bars show SE ($n = 12$). Asterisks indicate significant differences (**, $P < 0.01$) compared with nonsupplemented one-quarter-strength potato dextrose broth (PDB).

to infection as purple *Del/Ros1* fruit. However, *SlDFR*-silenced tomatoes lost this resistance and became as susceptible as the red sectors of VIGS-*Del/Ros1* fruit (Fig. 9A). Silencing of *SlF3H* also increased susceptibility to *B. cinerea*, although this remained lower than that of red sectors of VIGS-*SlDFR* fruit (Fig. 9A). This might be due to the impaired ripening observed in VIGS-*SlF3H* fruit.

Compared with purple *Del/Ros1* MoneyMaker tomatoes, the silenced sectors of VIGS-*SlDFR* fruit lost most of their anthocyanins (delphinidin derivatives and petunidin derivatives). This indicated that delphinidin and petunidin derivatives in purple tomatoes contribute specifically to the reduced susceptibility to *B. cinerea*, because the pathogen resistance of the *SlDFR*-silenced sectors was abolished. In contrast, although the silenced sectors of VIGS-*SlANS* fruit lost most of their anthocyanins (Supplemental Fig. S4A), they also accumulated increased amounts of myricetin derivatives (Supplemental Fig. S4B) and still showed good resistance to *B. cinerea* (Fig. 9A), suggesting that myricetin derivatives in tomato also contribute to reducing susceptibility to *B. cinerea*.

Natural Mutants Confirm the Importance of Specific Flavonoid Compounds to Susceptibility to *B. cinerea*

To confirm our results from *B. cinerea* infection of silenced sectors of VIGS-*SlDFR* and VIGS-*SlANS* fruit, we investigated the $aw^{-/-}$ *Del/Ros1* and $ae^{-/-}$ *Del/Ros1* lines selected in the F2 generation from *aw* (LA3281) and *ae* (LA3612) mutants crossed with the *Del/Ros1* tomato line.

When different fruit were inoculated with *B. cinerea* spores, the infection lesions on $ae^{-/-}$ *Del/Ros1* fruit were significantly smaller than those on wild-type and $aw^{-/-}$ *Del/Ros1* fruit at 3 dpi and were of equivalent size to those on *Del/Ros1* fruit at 3 dpi. This indicated that $ae^{-/-}$ *Del/Ros1* fruit had low susceptibly to *B. cinerea* while $aw^{-/-}$ *Del/Ros1* fruit lost most of their resistance compared with *Del/Ros1* fruit (Fig. 9B). These results, combined with the results from fruit VIGS, confirmed that silencing of DFR activity in purple tomatoes increased susceptibility to *B. cinerea* whereas silencing of ANS activity did not. The $ae^{-/-}$ *Del/Ros1* fruit accumulate myricetin derivatives (Supplemental Fig. S6) and have reduced susceptibility to *B. cinerea* infection. These data
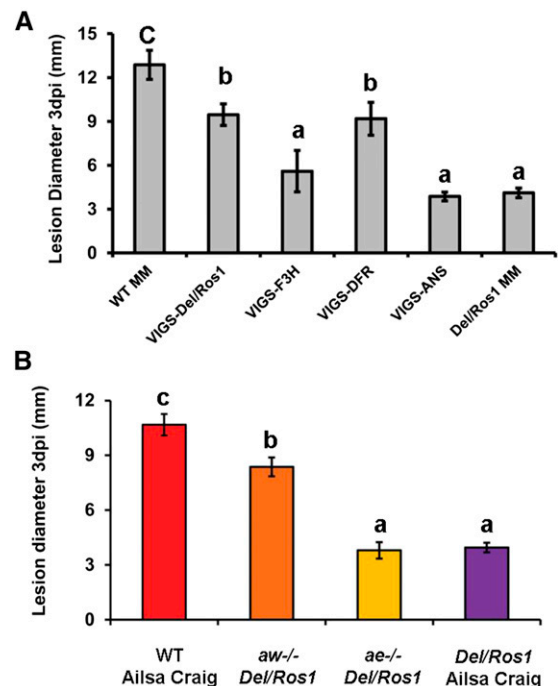
Figure 9. Blocking anthocyanin biosynthesis in *Del/Ros1* tomato using VIGS and natural mutants alters the susceptibility to *B. cinerea*. A, Susceptibility of different VIGS fruit to *B. cinerea* infection. Fruit were harvested at 14 d post breaker. For VIGS fruit, infection was done on silenced sectors. Lesion diameters were measured at 3 dpi. Error bars indicate SE ($n = 10$). Different letters indicate significantly different lesion size values at $P < 0.05$ (one-way ANOVA, Tukey's posthoc test). B, Susceptibility of different fruit to *B. cinerea* infection. Fruit were harvested at 14 d post breaker. Lesion diameters were measured at 3 dpi. Error bars indicate SE ($n = 10$). Different letters indicate significantly different values at $P < 0.05$ (one-way ANOVA, Tukey's posthoc test). MM, MoneyMaker; WT, wild type.

Figure 10. The superoxide-scavenging ability of flavonoid compounds is associated with the number of –OH groups on the B-ring and determines the roles of flavonoids in the susceptibility of tomato fruit to *B. cinerea*. A, Structures of different flavonoid compounds in tomato. B, Effects of flavonoid supp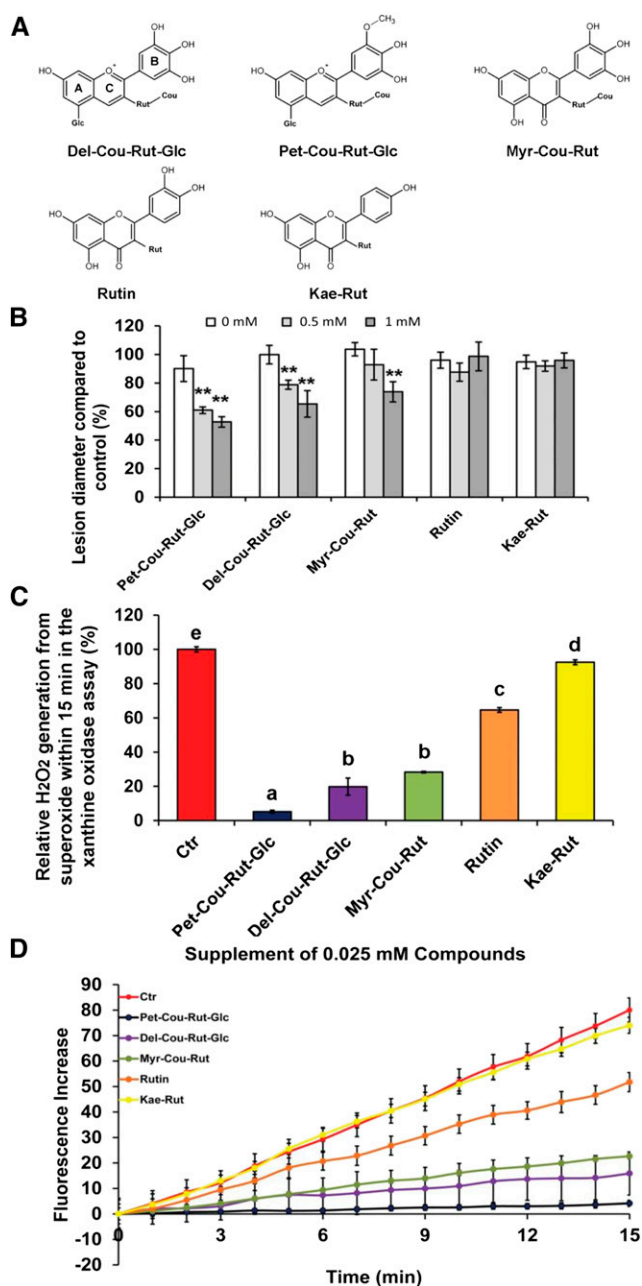lements to *B. cinerea* inocula on lesion size in wild-type tomato fruit. Purified flavonoids at different concentrations, as well as a control treatment (0 mM compound and 1% methanol [MeOH]), were supplied to different *B. cinerea* inoculation sites on the same fruit. Data are presented as the ratio of lesion diameter to the average lesion diameter of normal treatments (10 μL of B05.10 at 1.25×10^5 mL^{-1} in one-quarter-strength PDB). Error bars show SE ($n = 6$). Asterisks indicate significant differences between the tested concentration and the PDB control (**, $P < 0.01$) in Student's *t* test. For comparison, the maximum concentrations of Pet-Cou-Rut-Glc are about 0.8 and 3.4 mM in *Del/Ros1* and Indigo tomatoes, respectively. Maximum concentrations of Del-Cou-Rut-Glc are about 0.6 and 2.8 mM in *Del/Ros1*

suggest that myricetin derivatives, as well as delphinidin and petunidin derivatives, can contribute to resistance to *B. cinerea* in tomato fruit.

Decoration of the B-Ring Affects the Ability of Flavonoids to Scavenge Specific Free Radicals and Their Capacity to Decrease Susceptibility to *B. cinerea* Infection

It has been shown that the structure of flavonoids influences their ability to scavenge different free radicals (Wang et al., 2006; Markovic et al., 2014). It has been reported that quercetin is a better superoxide scavenger than kaempferol, whereas the ability of kaempferol to scavenge hydroxyl radicals is better than that of quercetin (Markovic et al., 2014). This suggests that the number of hydroxyl groups on the B-ring differentially affects how well flavonoids scavenge different free radicals. Compared with kaempferol, which has only one –OH on the 4′ position of the B-ring, compounds such as quercetin and its derivatives have an extra –OH on the C-3′ position of the B-ring; consequently, they have higher scavenging ability. Among the different positions of hydroxyl groups in flavonoids, a free –OH on the C-3′ position of the B-ring is believed to be the most powerful group contributing to scavenging ability (Burda and Oleszek, 2001). Myricetin has three hydroxyl groups in cis on its B-ring, further increasing its ability to act as an antioxidant (Fig. 10A). However, most of the tests on the abilities of flavonoids to scavenge free radicals have been done on aglycones, and other types of decoration (glycosylation, methylation,

and Indigo tomatoes, respectively. For myricetin derivatives, the maximum concentration found in Indigo tomatoes is about 0.6 mM. The maximum concentrations of Kae-Rut in *AtMYB12* tomatoes is about 4.8 mM, and the maximum rutin content in *AtMYB12* tomatoes is about 2.4 mM. Calculations were made based on data shown in Supplemental Table S1 (assuming that 1 g fresh weight of tomato is equivalent to 1 mL). C, Data for superoxide scavenging by tomato flavonoids. Suppression of the increase in fluorescence when different flavonoids were added to the xanthine oxidase reaction was assayed. Different flavonoids purified from tomatoes were added at 0.025 mM to the xanthine oxidase assay. For each compound, the fluorescence increase compared with initial fluorescence over a 15-min reaction time was calculated. Error bars show SE ($n = 3$). Different letters indicate significantly different values at $P < 0.05$ (one-way ANOVA, Tukey's posthoc test). D, Superoxide scavenging by different tomato flavonoids. The superoxide-scavenging assay was set up using the Amplex Red Xanthine/Xanthine Oxidase Assay Kit (Life Technologies). Xanthine oxidase catalyzes the oxidation of purine bases of xanthine to uric acid and superoxide. Superoxide spontaneously degrades to H_2O_2, which, in the presence of horseradish peroxidase, reacts with the Amplex Red reagent to generate resorufin. The presence of resorufin can be detected by fluorescence. Fluorescence was measured every 1 min for 15 min by a Varioskan Flash Multimode Reader (Thermo Scientific) using excitation at 560 nm and emission detection at 590 nm. For each sample, a blank control (Ctr) without xanthine was also measured at the same time. For each time point, background fluorescence was corrected by subtracting the value derived from the no-xanthine control. Error bars show SE ($n = 6$).

and acylation) affect the abilities of flavonoids and other antioxidants to scavenge different free radicals.

To investigate the effects of different flavonoids in tomato on susceptibility to *B. cinerea*, pure rutin (quercetin-3-*O*-rutinoside), one of the major flavonoids produced in tomato fruit, was purchased. The two major anthocyanins, delphinidin 3-*O*-(coumaroyl) rutinoside, 5-*O*-glucoside (Del-Cou-Rut-Glc) and petunidin 3-*O*-(coumaroyl) rutinoside, 5-*O*-glucoside (Pet-Cou-Rut-Glc), present in purple tomatoes were purified from the *Del/Ros1* purple tomatoes by HPLC purification, the major tomato flavonol, myricetin 3-*O*-(coumaroyl) rutinoside (Myr-Cou-Rut), was purified from *ae*$^{-/-}$ *Del/Ros1* fruit, and Kae-Rut was purified from *AtMYB12* tomatoes (see "Materials and Methods"; Supplemental Fig. S9). To screen for those compounds that influence susceptibility to *B. cinerea*, pure compounds at different concentrations were supplied to inoculation sites on wild-type tomatoes.

Supplementation with the two anthocyanins purified from tomato, as well as with the myricetin derivative (Myr-Cou-Rut), showed dose-dependent inhibition of *B. cinerea* lesion development. For the Kae-Rut and rutin supplements, no significant inhibition was seen at a final concentration of 1 mM (Fig. 10B). These data indicate that specific anthocyanins, as well as myricetin derivatives, can reduce the susceptibility of tomato fruit to *B. cinerea* infection.

In vitro growth assays showed that supplementation of these purified flavonoids/phenylpropanoids in medium did not inhibit the normal germination or germ-tube growth of *B. cinerea* on plates (Supplemental Figs. S10 and S11). This indicated that the effects of these compounds on *B. cinerea* infection were not due to the direct inhibition of growth of the fungus.

The Differential Activities of Different Flavonoids to Scavenge Superoxide Determines Their Ability to Reduce Susceptibility to *B. cinerea*

Previous data indicated that the ROS burst contributes negatively to the resistance to *B. cinerea* infection (Govrin and Levine, 2000; Zhang et al., 2013). Flavonoid compounds with –OH groups on the C-3′ position of the B-ring have been reported to have higher superoxide-scavenging ability (Rice-Evans et al., 1996). The ROS burst is initiated by the activity of NADPH oxidases, in the case of *B. cinerea* infection provided by both the host and the pathogen. The product of NADPH oxidase is superoxide, which is highly reactive and converted either spontaneously or by superoxide dismutases to H_2O_2. As H_2O_2 has a significantly longer half-life than superoxide, the spreading of the ROS burst to adjacent cells around the infection site is likely attributable to H_2O_2.

We tested the capacities of different flavonoids isolated from tomato to scavenge superoxide specifically using a xanthine oxidase assay (see "Materials and Methods"). Significant differences in superoxide scavenging were observed between equimolar concentrations of the different flavonoids (Fig. 10, C and D). Superoxide scavenging by kaempferol rutinoside, the predominant flavonoid in *AtMYB12* tomatoes, was not significantly greater than the addition of no antioxidant in the xanthine oxidase assay. Superoxide scavenging by Myr-Cou-Rut, Del-Cou-Rut-Glc, and Pet-Cou-Rut-Glc was significantly greater than that for Kae-Rut (Fig. 10, C and D). Rutin had a superoxide-scavenging ability intermediate between Kae-Rut and Myr-Cou-Rut. This suggested that the number of –OH groups or methoxylated groups on the B-ring primarily determines the superoxide-scavenging ability of flavonoids, which affects ROS dynamics during *B. cinerea* infection, as shown by the loss of the spreading distribution of ROS in infected fruit accumulating delphinidin, petunidin, and myricetin derivatives but not in those accumulating kaempferol derivatives (Fig. 7A). Therefore, there is a strong association between the structure of flavonoids, their ability to scavenge superoxide, and their ability to inhibit *B. cinerea* infection of living tissues. Interestingly, methylation of the 3′ hydroxyl group in petunidin 3-*O*-(coumaroyl) rutinoside, 5-*O*-glucoside did not reduce superoxide scavenging compared with nonmethylated Del-Cou-Rut-Glc (Fig. 10, C and D).

The presence of coumaroyl groups decorating those anthocyanins and flavonols that decrease susceptibility to *B. cinerea* might also contribute to the superoxide-scavenging abilities of the flavonoids that accumulate in the fruit of the different tomato lines. To identify whether coumaroylation is a major factor determining the effects of flavonoids on pathogen susceptibility, we purchased myricetin-3-*O*-rhamnoside (Myr-Rha) to compare with the acylated flavonoids purified from tomato fruit. The major differences between Myr-Cou-Rut, found in tomato fruit, and Myr-Rha are the glycosylation and absence of coumaroylation on the sugar attached to the C-ring (Supplemental Fig. S12A). There was no significant difference between Myr-Rha and Myr-Cou-Rut in superoxide-scavenging ability measured by the xanthine oxidase assay or on effects on *B. cinerea* growth or the susceptibility of fruit to *B. cinerea* infection (Supplemental Fig. S12, B–E). These data indicate that it is the –OH groups or the methoxylated groups on the B-ring that determine the superoxide-scavenging ability of flavonoids as well as their individual roles in susceptibility to *B. cinerea* in tomato fruit. The presence of acyl groups on the sugars attached to the C-ring appears to have little influence on the ability of flavonols to reduce susceptibility to *B. cinerea*.

DISCUSSION

AtMYB12 Tomato Fruit Show Delayed Overripening

Tomato fruit with higher antioxidant capacities show slower overripening (Bassolino et al., 2013; Zhang et al., 2013). *AtMYB12* tomatoes have increased levels of flavonols, and their antioxidant capacity is about 3 times higher than that of wild-type tomatoes (Luo et al.,

2008). At the beginning of overripening, *AtMYB12* tomatoes show slower overripening than wild-type fruit (Fig. 2). This is tightly correlated to their higher total antioxidant capacity as measured by the TEAC assay. However, the effect of flavonols in orange *AtMYB12* fruit was not as durable as the effect of anthocyanins in purple *Del/Ros1* tomatoes. After 3 to 4 weeks of storage (6 weeks after breaker), there were significant reductions in hydrophilic antioxidant capacity and increased production of MDA in *AtMYB12* tomato fruit (Supplemental Fig. S2). The high-anthocyanin/high-flavonol Indigo fruit had a longer, durable shelf life, indicating that durability is a dominant attribute conferred by anthocyanins, rather than the rapid softening of fruit, late in overripening, being a dominant trait conferred by flavonols. The reasons for the rapid loss of hydrophilic antioxidant capacity late in ripening in orange *AtMYB12* tomatoes need to be investigated further.

High Hydrophilic Antioxidant Capacity Is the Factor Determining Delayed Overripening

In both VIGS fruit and storage tests of natural mutants, a strong correlation was found between the length of overripening and the total antioxidant capacity of fruit (Fig. 5). When compared within the same genetic background, fruit with higher total antioxidant capacity could be stored longer than those with lower antioxidant capacities (Figs. 3–5).

We suggest that oxidative stress is a key factor in determining the rate of overripening of tomato fruit. During normal fruit ripening, the levels of ROS increase as fruit undergo different metabolic and physiological changes. Once oxidative stress reaches a certain level, at which point the scavenging systems can no longer work effectively, oxidative damage will begin. As oxidative damage reaches this critical point, it can directly cause cell damage and leakage and accompanying fruit softening (via lipid peroxidation and membrane damage) or indirectly (via ROS signaling) trigger downstream pathways that accelerate overripening (Zhang et al., 2013). For fruit with low antioxidant capacity, free radicals accumulate rapidly postbreaker (Supplemental Fig. S2; Mondal et al., 2004); thus, overripening proceeds strongly and quickly. Fruit with higher hydrophilic antioxidant capacity have a greater ability to scavenge free radicals and to reduce oxidative stress. Therefore, in these fruit, oxidative damage accumulates more slowly and overripening is delayed and weaker (Fig. 5).

AtMYB12 Fruit Show Low or No Capacity to Alter ROS Dynamics during *B. cinerea* Infection

Despite showing slower overripening than control tomatoes, *AtMYB12* tomatoes showed no reduced susceptibility to infection by *B. cinerea*. RT-qPCR results indicated that there was no significant difference in the expression of pathogen response genes between

wild-type and *AtMYB12* tomato fruit. The expression of the HR response gene *SlHSR203* was highly induced in wild-type and *AtMYB12* tomatoes after *B. cinerea* inoculation (Supplemental Fig. S8). Activation of *HSR203* is correlated with programmed cell death triggered by the HR (Pontier et al., 1998). Our data suggested that *AtMYB12* tomatoes have a stronger HR response to *B. cinerea* infection than anthocyanin-enriched *Del/Ros1* tomatoes. 3,3′-Diaminobenzidine staining confirmed that *AtMYB12* tomatoes showed no alterations in ROS dynamics compared with wild-type tomatoes, while *Del/Ros1* and Indigo tomatoes showed restricted, nonspreading ROS induction around infection sites. In addition, pretreatment with a ROS inhibitor could reduce the susceptibility of *AtMYB12* fruit to *B. cinerea*. Treatment with a ROS inducer increased fruit susceptibility to *B. cinerea* (Fig. 7B). These data imply an important role for ROS dynamics in the infection of ripe fruit by *B. cinerea*.

The ROS burst contributes positively to susceptibility to *B. cinerea* (Govrin and Levine, 2000). HR responses triggered by the ROS burst provide an efficient way for plants to resist biotrophic pathogens, but necrotrophic pathogens such as *B. cinerea* benefit from the death of host cells (Glazebrook, 2005). During infection, necrotrophic pathogens can even produce effectors to activate the ROS burst to promote pathogenesis (Kim et al., 2008; Alkan et al., 2009), and *B. cinerea* carries its own genes encoding NADPH oxidase whose activity is necessary for infection (Segmüller et al., 2008). Previous data showed that tomato fruit that have high anthocyanin contents can alter ROS dynamics by limiting the spread of ROS between cells during *B. cinerea* infection, thus suppressing lesion development (Zhang et al., 2013). For *AtMYB12*, although the total hydrophilic antioxidant capacity of the fruit is high, the ability of the specific flavonols that accumulate to quench any spread of the ROS burst is low (Fig. 7A). This indicates that, unlike the delay in overripening, the impact of flavonoids on the ROS burst during pathogen infection is not determined by their total antioxidant capacity but, instead, by the specific scavenging activity of the different flavonoids.

Decoration of the B-Ring of Flavonoids Is Linked to the Susceptibility of Fruit to *B. cinerea*

Using VIGS and natural mutants, we have shown that silencing of *DFR* and *ANS* has different effects on susceptibility to *B. cinerea* in *Del/Ros1* tomatoes (Fig. 9). Silencing of *SlANS* in *Del/Ros1* tomatoes reduced the production of anthocyanins in silenced sectors but also showed low susceptibility to *B. cinerea*. LC-MS data indicated that myricetin derivatives, a group of flavonols that have three –OH groups on the B-ring, accumulated in VIGS-*SlANS* tomatoes, due to the induction of *SlF3′5′H* expression in VIGS-*SlANS* fruit.

Purple tomato fruit are enriched with delphinidin 3-*O*-(coumaroyl)-rutinoside, 5-*O*-glucoside and petunidin

3-*O*-(coumaroyl)-rutinoside, 5-*O*-glucoside (delphinidin has three –OH groups on its B-ring and petunidin has two –OH groups and one methoxylated group on its B-ring). In *aw*$^{-/-}$ *Del/Ros1* fruit, kaempferol derivatives (with just one –OH group on the B-ring and no coumaroyl group) are enriched (Supplemental Fig. S4). In the *ae*$^{-/-}$ *Del/Ros1* mutant, although anthocyanins are missing, the content of myricetin derivatives (three –OHs on the B-ring) is increased as a result of the induction of F3′5′H expression (Supplemental Figs. S3 and S6). Like the VIGS fruit, *aw*$^{-/-}$ *Del/Ros1* Ailsa Craig fruit are susceptible *to B. cinerea*, while *ae*$^{-/-}$ *Del/Ros1* fruit show reduced susceptibility. Consequently, the number of –OH groups, or methoxylated groups, on the B-rings of the flavonoids that accumulate is associated with susceptibility to *B. cinerea*. Flavonoids have been shown to differ with respect to their ability to scavenge different free radical species, dependent on their structure. Markovic et al. (2014) showed that quercetin scavenges superoxide radicals better than kaempferol, although Wang et al. (2006) showed the reverse capabilities, with myricetin poorer at scavenging superoxide than kaempferol. However, Wang et al. (2006) also found myricetin and quercetin more effective than kaempferol in quenching the ROS burst in human polymorphonuclear neutrophils. Both these studies used pure flavonol aglycones, which are present in only trace amounts in most plant tissues.

The ROS burst in both plants and animals is generated by the activity of the NADPH oxidase complex, which forms superoxide that subsequently may be dismuted either spontaneously or catalytically, by superoxide dismutase, to form H_2O_2. Our data from direct assays of superoxide scavenging by the differentially decorated flavonoids that accumulate in different tomato lines (for which susceptibility to *B. cinerea* has been measured) show that flavonoids from tomato with more –OH groups on their B-ring have superior superoxide-scavenging abilities (Fig. 10, C and D). Interestingly, substitution of one hydroxyl group on the B-ring with a methyl group in Pet-Cou-Rut-Glc did not reduce superoxide-scavenging ability compared with the nonmethylated Del-Cou-Rut-Glc (Fig. 10, C and D), suggesting that decoration of the 3′ position, rather than the chemical identity of the group at this position, is important for scavenging superoxide.

In tomato, reduced susceptibility to *B. cinerea* appears to involve specific flavonoid compounds. The accumulation of flavonoid compounds with three –OH groups (or two and one methoxylated group) on their B-ring decreases the susceptibility of tomato to *B. cinerea* by suppressing the spread of the ROS burst following infection. This probably involves the flavonoids quenching the superoxide produced by the NADPH oxidase effectively, preventing the production of longer lived H_2O_2 that can kill the surrounding cells, allowing *B. cinerea* to invade.

CONCLUSION

The general antioxidant capacity of fleshy fruit can be enhanced by different breeding or bioengineering strategies (Rousseaux et al., 2005; Nambeesan et al., 2010; Minas et al., 2012; Zidenga et al., 2012; Zhang et al., 2013). Our results show that increasing the total antioxidant capacity of tomato is an efficient way to delay the overripening of fruit. Therefore, breeding and bioengineering strategies targeting general antioxidant capacity could offer effective approaches to improve the shelf life of fleshy fruit in general.

In contrast, the structure of specific flavonoids is important in determining the susceptibility of fruit to *B. cinerea* infection, which is an important component of the shelf-life quality trait. The number of horticultural crops synthesizing flavonoids with three –OH groups on the B-ring is relatively small (grape [*Vitis vinifera*], eggplant [*Solanum melongena*], and black currant [*Ribes nigrum*] are examples) and dependent on the activity of F3′5′H, which is absent from many plant species (Nielsen et al., 2003; Sadilova et al., 2006; He et al., 2010). However, the information we have derived from investigating the effects of specific flavonoids on susceptibility to *B. cinerea* in the model fleshy fruit tomato could be applied in selecting lower susceptibility varieties of grape, which are well characterized for their contents of myricetin, quercetin, kaempferol, cyanidin, delphinidin, petunidin, malvidin, and peonidin derivatives (Mattivi et al., 2006). For species that lack the gene encoding F3′5′H activity, such as strawberry (*Fragaria* spp. [and other Rosaceae]; Wessinger and Rausher, 2012), genetic modification strategies could be considered as a means to reduce the susceptibility of fruit to *B. cinerea*. Our findings provide mechanistic insight for new strategies to improve the shelf life of tomato as well as other fleshy fruit.

MATERIALS AND METHODS

Plant Materials

The *AtMYB12* tomato (*Solanum lycopersicum*), in which the expression of the MYB12 transcription factor from Arabidopsis (*Arabidopsis thaliana*) is driven fruit specifically from breaker onward by the E8 promoter (Deikman et al., 1992), has been described by Luo et al. (2008). A new line of tomato in the MicroTom genetic background was made by crossing *Del/Ros1* N MicroTom (Butelli et al., 2008) with *AtMYB12* MicroTom. The resulting line, named Indigo, contains high amounts of both anthocyanins and flavonols. Two natural mutants of tomato, *aw* (LA3736) and *ae* (LA3612), in the Ailsa Craig genetic background were obtained from the Tomato Genetic Resource Center (http://tgrc.ucdavis.edu/). The *aw* mutant lacks DFR activity (Goldsbrough et al., 1994), while the *ae* mutant is deficient in ANS activity (Tanksley et al., 1992; De Jong et al., 2004). Both *aw* and *ae* mutants were crossed with *Del/Ros1* N MicroTom tomato (Butelli et al., 2008). The *aw*$^{-/-}$ *Del/Ros1* and *ae*$^{-/-}$ *Del/Ros1* lines were selected from a segregating F2 population. Controls (with functional *Aw* and *Ae* genes) carrying *Del/Ros1* were also selected from these F2 populations.

Storage Tests

Storage tests for tomatoes in the MicroTom genetic background were undertaken as described previously (Zhang et al., 2013) following a protocol used extensively to measure shelf life in the tomato industry. Red wild-type, purple *Del/Ros1*, orange *AtMYB12*, and Indigo (*Del/Ros1;AtMYB12*) tomatoes were tagged at breaker and harvested 2 weeks after breaker. Fruit was washed with water and sterilized with 10% (v/v) bleach for 20 min. After surface sterilization, fruit were rinsed three times with sterilized water and air dried in a clean flow cabinet. Ten fruit from the same line were placed in one clean Phytatray II

(Sigma-Aldrich) and stored in the dark at 17°C. Each week, the proportion of fruit showing the symptoms of overripening (visual softening and collapse of the surface) was calculated for each box, and the fresh weight was measured. After inspection, the fruit were transferred to a new Phytatray.

TEAC Assay

The TEAC assay for fruit antioxidant capacity was performed as described previously (Butelli et al., 2008). For juice antioxidant activity tests, tomato fruit were harvested at 2 weeks after breaker. Fruit were blended in a metal blender. After centrifugation, supernatants were taken for TEAC measurement.

Xanthine Oxidase Assay of Superoxide Scavenging

The superoxide-scavenging assay was set up using the Amplex Red Xanthine/Xanthine Oxidase Assay Kit (Life Technologies). Xanthine oxidase catalyzes the oxidation of purine bases of xanthine to uric acid and superoxide. Superoxide spontaneously degrades to H_2O_2, which, in the presence of horseradish peroxidase, reacts with the Amplex Red reagent to generate resorufin. The presence of resorufin can be detected by fluorescence. To test the scavenging ability of different flavonoids, purified compounds were added at 0.025 mM to 100-μL reactions (50 μM Amplex Red, 0.2 units mL^{-1} horseradish peroxidase, 100 μM xanthine, and 200 microunits of xanthine oxidase) on 96-well plates. The reactions were maintained at 37°C. Fluorescence was measured every 1 min for 15 min by a Varioskan Flash Multimode Reader (Thermo Scientific) using excitation at 560 nm and emission detection at 590 nm. For each sample, a blank control without xanthine was also measured at the same time. For each time point, background fluorescence was corrected by subtracting the value derived from the no-xanthine control.

MDA Measurements

Tomato fruit at different ripening stages were harvested and washed. Seeds were removed from tomato fruit, and 2.5 g of fruit at the same stage of ripeness were ground in 10 mL of 10 mM sodium phosphate buffer, pH 7.2 (adding acid-purified sand to assist homogenization). MDA measurement was done as described previously (Tamagnone et al., 1998; Zhang et al., 2013).

Botrytis cinerea Growth and Inoculation

The *B. cinerea* strain B05.10 was used for all in planta studies and in vitro assays for growth on agar plates and germination. The B05.10-derived strain OliCBcGFP constitutively expresses BcGFP1, a synthetic variant of enhanced GFP with codon usage optimized for *B. cinerea* (Leroch et al., 2011), was kindly provided by M. Leroch and M. Hahn (University of Kaiserslautern) and has been used for in vitro growth assays in liquid medium.

Culture of *B. cinerea* and collection of spores were done as described previously (Stefanato et al., 2009; Zhang et al., 2013); inoculum was prepared in one-quarter-strength PDB (6 g L^{-1}). For spray inoculation, tomato fruit were harvested 14 d after breaker and surface sterilized. Intact fruit were sprayed thoroughly with spores (2.5×10^5 spores mL^{-1}) three times and kept at 20°C in high humidity. Infection symptoms were monitored at 3, 4, and 5 dpi.

For wound inoculation, surface-sterilized fruit were wounded by 200-μL Eppendorf tips. The fungal culture was diluted with one-quarter-strength PDB to 5×10^4 spores mL^{-1} (for MicroTom fruit) or 1×10^5 spores mL^{-1} (for MoneyMaker fruit) and inoculated for 1.5 h to stimulate germination. The spore inoculum (5 μL) was added to each wound. Lesion diameter was measured 24, 48, and 72 h after inoculation.

Plate Assay for Growth of *B. cinerea*

The direct effect of purified compounds on the germination and growth of *B. cinerea* was tested in a 96-well assay adapted from Schoonbeek et al. (2001). For germination assays, B05.10 was distributed over a 96-well plate (Greiner) at a concentration of 5×10^3 spores per well in 100 μL of one-quarter-strength PDB supplemented with the test compound and a final concentration of 1% (v/v) MeOH. Spores were incubated for 16 h at 21°C and photographed using an inverted microscope (Zeiss Axiovert25, with a Canon EOS D30 camera). For growth assays, OliCBcGFP spores were placed on a 96-well plate (Greiner) at a concentration of 1.5×10^4 spores per well in 100 μL of one-half-strength PDB supplemented with the test compound and a final concentration of 1% MeOH

and incubated at 21°C. Fluorescence was measured at 535 nm after excitation at 485 nm on a plate reader (Varioskan; Thermo Scientific). Growth was determined as fold increase of the GFP fluorescence between 1 and 24 h post inoculation, representative of the increase of living *B. cinerea* tissue.

VIGS

The Gateway destination vector pTRV2-GW was kindly provided by Dr. Diego Orzaez (Orzaez et al., 2009). Fragments of target genes (200–300 bp of the complementary DNA; for primers, see Supplemental Table S1) were amplified with Gateway-compatible primers and recombined into pDONR207 by the BP reaction to generate an entry clone. The entry vector was then recombined with the pTRV2-GW destination vector using an LR reaction to make VIGS clones pTRV2-*SlF3H*, pTRV2-*SlDFR*, and pTRV2-*SlANS*. The sequenced VIGS vectors were then transferred into *Agrobacterium tumefaciens* strain GV3101:pMP90 by electroporation.

Agroinfiltration was performed as described previously (Orzaez et al., 2009; Zhang et al., 2013). Agroinfiltrated fruit were marked at the breaker stage, and samples were collected at 2 weeks after breaker. Primers for qPCR check are shown in Supplemental Table S2.

Supplementation of Tomato Juice with Different Flavonoids during Inoculation of *B. cinerea*

For juice supplementation, *B. cinerea* spores were first diluted to 1.25×10^6 spores mL^{-1} in one-quarter-strength PDB and incubated at room temperature for 2 h. One volume of this initial culture was mixed with 9 volumes of juice prepared from wild-type, *AtMYB12*, *Del/Ros1*, and Indigo tomatoes (to make the final concentration to 1.25×10^5 spores mL^{-1}). As a control, 1 volume of the initial culture was mixed with 9 volumes of one-quarter-strength PDB. Six wound sites were made on each wild-type MoneyMaker fruit, and each site was inoculated with 10 μL of juice plus *B. cinerea* culture. Inoculated fruit were stored in boxes with high humidity. Every 24 h, 10 μL of juice (or water for controls) was added to the inoculation site. Lesion sizes were assessed at 3 dpi.

For supplementation with specific compounds, the *B. cinerea* culture was diluted to 1.25×10^5 spores mL^{-1} in one-quarter-strength PDB supplemented with purified compounds to different final concentrations (for the control, 5% (v/v) ethanol was added to one-quarter-strength PDB). Culture (10 μL) was inoculated onto each site. Solutions of compounds in water (10 μL) were supplied to the inoculation sites every 24 h. Lesion sizes were assessed at 3 dpi.

Isolation of Phenolic Compounds and Analysis by LC-MS

Sectors of VIGS fruit or mutants were ground into fine powder in liquid nitrogen. To isolate phenolic compounds, 1 g of ground tissue was extracted in 10 mL of 50% (v/v) MeOH (containing 2% [v/v] formic acid) in the dark, at 4°C, overnight with gentle agitation (30 rpm). Samples were then centrifuged for 10 min at 4,000 rpm at 4°C. Supernatants were collected and then cleared by filtration through a 0.22-μm membrane filter (Millipore). Anthocyanins and flavonoids were analyzed on an Agilent Technologies 1100 HPLC device attached to a single-quadrupole mass spectrometer. Separation was on a 100- $\times$ 2.1- mm 2.6μ Kinetex XB-C18 column (Phenomenex) using the following gradient of acetonitrile (ACN; solvent B) versus 0.1% (v/v) formic acid in water (solvent A), run at 300 μL min^{-1} and 25°C: 0 to 1 min, 2% B; 6 min, 10% B; 26 min, 30% B; 36.5 min, 90% B; 37.5 min, 90% B; 38 min, 2% B; and 45 min, 2% B. Peaks were detected by UV/visible light absorbance, collecting chromatograms at 280, 320, 370, and 525 nm. Peaks were also detected by positive electrospray mass spectrometry, collecting spectra from mass-to-charge ratio (m/z) 100 to 1,200 with ramped fragmentor voltage. Spray chamber conditions were 11.5 L min^{-1} drying gas at 350°C, 25 p.s.i. nebulizer pressure, and a spray voltage of 4,000 V. To confirm the identity of peaks, samples were also run on a Surveyor HPLC device equipped with a Deca XPplus ion-trap mass spectrometer, using the same column, solvent system, and gradient. The mass spectrometer was set up to collect positive electrospray mass spectrometry spectra from m/z 100 to 2,000 and data-dependent tandem mass spectrometry spectra of the most abundant ions at an isolation width of m/z 4 and 35% collision energy. Spray chamber conditions were 350°C capillary temperature, 50 units of sheath gas, 5 units of auxiliary gas, and a spray voltage of 3.8 kV.

Purification of Flavonoid Compounds from Tomato Fruit

To purify major anthocyanins from *Del/Ros1* tomato, 1 g of freeze-dried fruit powder was extracted with 20 mL of 2% formic acid in 50% (v/v) MeOH. After

filtrating through Whatman No. 1 paper, polyphenol extracts were transferred to a rotary evaporator to remove all MeOH for subsequent transfer to a solid-phase 5,000-mg Chromabond C18 column (Macherey-Nagel). Flavonols were eluted with 60 mL of 2% formic acid in 60% (v/v) MeOH, followed by the elution of anthocyanins with 10 mL of 2% formic acid in 100% MeOH. Anthocyanin extracts were transferred to a rotary evaporator to remove all MeOH. The water solution was then frozen in liquid N_2 and freeze dried. The freeze-dried powder was weighed, and a sample (10 mg) was dissolved with 200 μL of 80% MeOH.

Anthocyanin extracts were run on a 250- × 30-mm i.d. Phenomenex 5 μm Gemini NX-C18 110 Å column using a Varian ProStar 210 preparative HPLC device (Agilent Technologies) connected to a Varian ProStar 410 AutoSampler (Agilent Technologies). Separation was achieved using a linear gradient of ACN versus 1.9% formic acid and 0.1% ammonium formate in water, run at 10 mL min^{-1} and 25°C: 0 min, 3% ACN; 8.5 min, 3% ACN; 100 min, 20% ACN; 133.5 min, 30% ACN; 150 min, 30% ACN; 153 min, 97% ACN; 165 min, 97% ACN; 167 min, 3% ACN; and 170 min, 3% ACN. The elution products were monitored with a photo diode array detector over the range of 200 to 600 nm. Anthocyanins or flavonoids were detected by light absorbance using collecting channels at 535 or 280 nm, respectively. The anthocyanins eluted after 50 min, and 10-mL fractions were collected every 1 min between 50 and 120 min.

Anthocyanin fractions obtained by Varian ProStar 210 preparative HPLC were further purified using a small-scale preparative HPLC device equipped with a smaller C18 column to achieve better separation. Samples were run on a 19- × 150-mm i.d. Waters 5-μm XBridge BEH C18 prep column (130Å) connected to a Prep 2000 HPLC system (Waters) with a UV/visible light detector (Waters). Separation was achieved using a linear gradient of ACN versus 1.9% formic acid and 0.1% ammonium formate in water, run at 4 mL min^{-1} and 25°C: 0 min, 3% ACN; 5 min, 3% ACN; 60 min, 20% ACN; 80 min, 30% ACN; 90 min, 30% ACN; 92 min, 97% ACN; 99 min, 97% ACN; and 100 min, 3% ACN. The elution products were monitored with a photo diode array detector over the range of 200 to 600 nm. Anthocyanins were detected by light absorbance using the collecting channel at 535 nm. The purified anthocyanins were concentrated using a nitrogen evaporator and resuspended in 50% (v/v) MeOH at 200 μM and stored at −80°C until further use.

Rutin (quercetin 3-O-rutinoside) was purchased from Sigma-Aldrich. To purify Kae-Rut and myricetin 3-O-(coumaroyl)-rutinoside, $AtMYB12$ fruit and $ae^{-/-}$ $Del/Ros1$ fruit were used, respectively. Preseparation was done as described for anthocyanins. The crude material was purified by HPLC on a Dionex Ultimate 3000 instrument equipped with a variable wavelength detector and a fraction collector using a C18 reverse-phase semipreparative column (Grace Vydac C18 Monomeric; 120 A, particle size of 5 μm, 250 × 10 mm). Separation was achieved using a linear gradient of ACN (solvent B) against 1.9% formic acid and 0.1% ammonium formate in water (solvent A), run at a flow rate 10 mL min^{-1} and 25°C: 0 min, 3% ACN; 2 min, 3% ACN; 18 min, 20% ACN; 20 min, 30% ACN; 22 min, 30% ACN; 25 min, 97% ACN; 27 min, 97% ACN; 29 min, 3% ACN; and 31 min, 3% ACN. The flavonoids were detected at 280 nm. Fractions were collected between 10 and 25 min only.

After purification, compounds were analyzed on a Surveyor HPLC system attached to a DecaXPplus ion-trap mass spectrometer (both Thermo Scientific) as described above, using 10-μL injections.

Statistics

For comparison of individual treatments with their relevant controls, unpaired two-tailed Student's t tests were used, and $P < 0.05$ was considered significant. To compare measurements of multiple treatments with each other and the control, we performed univariate ANOVA followed by the posthoc Tukey's test of multiple pairwise comparisons to determine group differences using Genstat version 16 (http://www.vsni.co.uk/). The χ^2 test was used to determine the effect of various treatments on the distribution of observations over different classes (e.g. susceptibility level; Fig. 2) and the proportion of ripe versus overripe fruit (Figs. 5B and 6B). Whenever counts in any of the classes in any of the treatments were zero, counts in every class were adjusted by adding a 1% value of total counts correction.

Supplemental Data

The following supplemental materials are available.

Supplemental Figure S1. Phenotypes of tomato fruit on the vine at different stages.

Supplemental Figure S2. The high antioxidant capacity of $AtMYB12$ tomatoes is not stable.

Supplemental Figure S3. VIGS of anthocyanin biosynthetic genes in $Del/Ros1$ tomatoes.

Supplemental Figure S4. VIGS fruit accumulate different flavonoid compounds.

Supplemental Figure S5. Compounds identified by LC-MS.

Supplemental Figure S6. HPLC profile of natural mutants crossed with $Del/Ros1$ tomato.

Supplemental Figure S7. $AtMYB12$ MoneyMaker tomatoes are susceptible to $B.$ $cinerea$.

Supplemental Figure S8. Expression of pathogen response genes following $B.$ $cinerea$ inoculation.

Supplemental Figure S9. Preparative HPLC to purify anthocyanins from $Del/Ros1$ tomato fruit.

Supplemental Figure S10. Effects of flavonoid derivatives on the growth of $B.$ $cinerea$.

Supplemental Figure S11. Effects of flavonoid derivatives on the germination of $B.$ $cinerea$.

Supplemental Figure S12. B-ring structure determines the scavenging ability of flavonoids.

Supplemental Table S1. Levels of major phenylpropanoids in the fruit of different tomato lines.

Supplemental Table S2. Primers used in this research.

LITERATURE CITED

Alkan N, Davydov O, Sagi M, Fluhr R, Prusky D (2009) Ammonium secretion by Colletotrichum coccodes activates host NADPH oxidase activity enhancing host cell death and fungal virulence in tomato fruits. Mol Plant Microbe Interact **22:** 1484–1491

Bassolino L, Zhang Y, Schoonbeek HJ, Kiferle C, Perata P, Martin C (2013) Accumulation of anthocyanins in tomato skin extends shelf life. New Phytol **200:** 650–655

Bhagwan A, Reddy YN, Rao PV, Mohankumar KC (2000) Shelf life extension of tomato fruits by postharvest antioxidant application. J Appl Hortic **2:** 88–91

Bovy A, de Vos R, Kemper M, Schijlen E, Almenar Pertejo M, Muir S, Collins G, Robinson S, Verhoeyen M, Hughes S, et al (2002) High-flavonol tomatoes resulting from the heterologous expression of the maize transcription factor genes LC and C1. Plant Cell **14:** 2509–2526

Burda S, Oleszek W (2001) Antioxidant and antiradical activities of flavonoids. J Agric Food Chem **49:** 2774–2779

Butelli E, Titta L, Giorgio M, Mock HP, Matros A, Peterek S, Schijlen EG, Hall RD, Bovy AG, Luo J, et al (2008) Enrichment of tomato fruit with health-promoting anthocyanins by expression of select transcription factors. Nat Biotechnol **26:** 1301–1308

Cantu D, Blanco-Ulate B, Yang L, Labavitch JM, Bennett AB, Powell AL (2009) Ripening-regulated susceptibility of tomato fruit to Botrytis cinerea requires NOR but not RIN or ethylene. Plant Physiol **150:** 1434–1449

Cantu D, Vicente AR, Greve LC, Dewey FM, Bennett AB, Labavitch JM, Powell AL (2008) The intersection between cell wall disassembly, ripening, and fruit susceptibility to Botrytis cinerea. Proc Natl Acad Sci USA **105:** 859–864

Centeno DC, Osorio S, Nunes-Nesi A, Bertolo AL, Carneiro RT, Araujo WL, Steinhauser MC, Michalska J, Rohrmann J, Geigenberger P, et al (2011) Malate plays a crucial role in starch metabolism, ripening, and soluble solid content of tomato fruit and affects postharvest softening. Plant Cell **23:** 162–184

Dean R, Van Kan JAL, Pretorius ZA, Hammond-Kosack KE, Di Pietro A, Spanu PD, Rudd JJ, Dickman M, Kahmann R, Ellis J, et al (2012) The top 10 fungal pathogens in molecular plant pathology. Mol Plant Pathol **13:** 414–430

Deikman J, Kline R, Fischer RL (1992) Organization of ripening and ethylene regulatory regions in a fruit-specific promoter from tomato (*Lycopersicon esculentum*). Plant Physiol 100: 2013–2017

De Jong WS, Eannetta NT, De Jong DM, Bodis M (2004) Candidate gene analysis of anthocyanin pigmentation loci in the Solanaceae. Theor Appl Genet 108: 423–432

Dhindsa RS, Plumb-Dhindsa P, Thorpe TA (1981) Leaf senescence: correlated with increased levels of membrane permeability and lipid peroxidation, and decreased levels of superoxide dismutase and catalase. J Exp Bot 32: 93–101

Glazebrook J (2005) Contrasting mechanisms of defense against biotrophic and necrotrophic pathogens. Annu Rev Phytopathol 43: 205–227

Goldsbrough A, Belzile F, Yoder JI (1994) Complementation of the tomato *anthocyanin without* (aw) mutant using the dihydroflavonol 4-reductase gene. Plant Physiol 105: 491–496

Govrin EM, Levine A (2000) The hypersensitive response facilitates plant infection by the necrotrophic pathogen Botrytis cinerea. Curr Biol 10: 751–757

He F, Mu L, Yan GL, Liang NN, Pan QH, Wang J, Reeves MJ, Duan CQ (2010) Biosynthesis of anthocyanins and their regulation in colored grapes. Molecules 15: 9057–9091

Heim KE, Tagliaferro AR, Bobilya DJ (2002) Flavonoid antioxidants: chemistry, metabolism and structure-activity relationships. J Nutr Biochem 13: 572–584

Holton TA, Brugliera F, Lester DR, Tanaka Y, Hyland CD, Menting JGT, Lu CY, Farcy E, Stevenson TW, Cornish EC (1993) Cloning and expression of cytochrome P450 genes controlling flower colour. Nature 366: 276–279

Jimenez A, Creissen G, Kular B, Firmin J, Robinson S, Verhoeyen M, Mullineaux P (2002) Changes in oxidative processes and components of the antioxidant system during tomato fruit ripening. Planta 214: 751–758

Kim KS, Min JY, Dickman MB (2008) Oxalic acid is an elicitor of plant programmed cell death during Sclerotinia sclerotiorum disease development. Mol Plant Microbe Interact 21: 605–612

Kopeliovitch E, Rabinowitch HD, Mizrahi Y, Kedar N (1979) The potential of ripening mutants for extending the storage life of the tomato fruit. Euphytica 28: 99–104

Kramer M, Sanders R, Bolkan H, Waters C, Sheeny RE, Hiatt WR (1992) Postharvest evaluation of transgenic tomatoes with reduced levels of polygalacturonase: processing, firmness and disease resistance. Postharvest Biol Technol 1: 241–255

Leroch M, Mernke D, Koppenhoefer D, Schneider P, Mosbach A, Doehlemann G, Hahn M (2011) Living colors in the gray mold pathogen Botrytis cinerea: codon-optimized genes encoding green fluorescent protein and mCherry, which exhibit bright fluorescence. Appl Environ Microbiol 77: 2887–2897

Luo J, Butelli E, Hill L, Parr A, Niggeweg R, Bailey P, Weisshaar B, Martin C (2008) AtMYB12 regulates caffeoyl quinic acid and flavonol synthesis in tomato: expression in fruit results in very high levels of both types of polyphenol. Plant J 56: 316–326

Markovic JMD, Milenkovic D, Amie D, Popovic-Bijelic A, Mojovic M, Pasti IA, Markovic ZS (2014) Energy requirements of the reactions of kaempferol and selected radical species in different media: towards the prediction of the possible radical scavenging mechanisms. Struct Chem 2: 1795–1804

Mattivi F, Guzzon R, Vrhovsek U, Stefanini M, Velasco R (2006) Metabolite profiling of grape: flavonols and anthocyanins. J Agric Food Chem 54: 7692–7702

Maul F, Sargent S, Balaban M, Baldwin E, Huber D, Sims C (1998) Aroma volatile profiles from ripe tomatoes are influenced by physiological maturity at harvest: an application for electronic nose technology. J Am Soc Hortic Sci 123: 1094–1101

Maul F, Sargent SA, Sims CA, Baldwin EA, Balaban MO, Huber DJ (2000) Tomato flavor and aroma quality as affected by storage temperature. J Food Sci 65: 1228–1237

Mehta RA, Cassol T, Li N, Ali N, Handa AK, Mattoo AK (2002) Engineered polyamine accumulation in tomato enhances phytonutrient content, juice quality, and vine life. Nat Biotechnol 20: 613–618

Meli VS, Ghosh S, Prabha TN, Chakraborty N, Chakraborty S, Datta A (2010) Enhancement of fruit shelf life by suppressing N-glycan processing enzymes. Proc Natl Acad Sci USA 107: 2413–2418

Minas IS, Tanou G, Belghazi M, Job D, Manganaris GA, Molassiotis A, Vasilakakis M (2012) Physiological and proteomic approaches to address the active role of ozone in kiwifruit post-harvest ripening. J Exp Bot 63: 2449–2464

Mondal K, Sharma NS, Malhotra SP, Dhawan K, Singh R (2004) Antioxidant systems in ripening tomato fruits. Biol Plant 48: 49–53

Muir SR, Collins GJ, Robinson S, Hughes S, Bovy A, Ric De Vos CH, van Tunen AJ, Verhoeyen ME (2001) Overexpression of petunia chalcone isomerase in tomato results in fruit containing increased levels of flavonols. Nat Biotechnol 19: 470–474

Mutschler MA, Wolfe DW, Cobb ED, Yourstone KS (1992) Tomato fruit quality and shelf life in hybrids heterozygous for the alc ripening mutant. HortScience 27: 352–355

Nambeesan S, Datsenka T, Ferruzzi MG, Malladi A, Mattoo AK, Handa AK (2010) Overexpression of yeast spermidine synthase impacts ripening, senescence and decay symptoms in tomato. Plant J 63: 836–847

Nielsen ILF, Haren GR, Magnussen EL, Dragsted LO, Rasmussen SE (2003) Quantification of anthocyanins in commercial black currant juices by simple high-performance liquid chromatography: investigation of their pH stability and antioxidative potency. J Agric Food Chem 51: 5861–5866

Olsen KM, Slimestad R, Lea US, Brede C, Løvdal T, Ruoff P, Verheul M, Lillo C (2009) Temperature and nitrogen effects on regulators and products of the flavonoid pathway: experimental and kinetic model studies. Plant Cell Environ 32: 286–299

Orzaez D, Medina A, Torre S, Fernández-Moreno JP, Rambla JL, Fernández-Del-Carmen A, Butelli E, Martin C, Granell A (2009) A visual reporter system for virus-induced gene silencing in tomato fruit based on anthocyanin accumulation. Plant Physiol 150: 1122–1134

Pontier D, Tronchet M, Rogowsky P, Lam E, Roby D (1998) Activation of hsr203, a plant gene expressed during incompatible plant-pathogen interactions, is correlated with programmed cell death. Mol Plant Microbe Interact 11: 544–554

Povero G, Gonzali S, Bassolino L, Mazzucato A, Perata P (2011) Transcriptional analysis in high-anthocyanin tomatoes reveals synergistic effect of Aft and atv genes. J Plant Physiol 168: 270–279

Rice-Evans CA, Miller NJ, Paganga G (1996) Structure-antioxidant activity relationships of flavonoids and phenolic acids. Free Radic Biol Med 20: 933–956

Rice-Evans CA, Miller NJ, Paganga G (1997) Antioxidant properties of phenolic compounds. Trends Plant Sci 2: 152–159

Rousseaux MC, Jones CM, Adams D, Chetelat R, Bennett A, Powell A (2005) QTL analysis of fruit antioxidants in tomato using Lycopersicon pennellii introgression lines. Theor Appl Genet 111: 1396–1408

Sadilova E, Stintzing FC, Carle R (2006) Anthocyanins, colour and antioxidant properties of eggplant (Solanum melongena L.) and violet pepper (Capsicum annuum L.) peel extracts. Z Naturforsch C 61: 527–535

Schoonbeek H, Del Sorbo G, De Waard MA (2001) The ABC transporter BcatrB affects the sensitivity of *Botrytis cinerea* to the phytoalexin resveratrol and the fungicide fenpiclonil. Mol Plant Microbe Interact 14: 562–571

Segmüller N, Kokkelink L, Giesbert S, Odinius D, van Kan J, Tudzynski P (2008) NADPH oxidases are involved in differentiation and pathogenicity in *Botrytis cinerea*. Mol Plant Microbe Interact 21: 808–819

Stefanato FL, Abou-Mansour E, Buchala A, Kretschmer M, Mosbach A, Hahn M, Bochet CG, Métraux JP, Schoonbeek HJ (2009) The ABC transporter BcatrB from Botrytis cinerea exports camalexin and is a virulence factor on Arabidopsis thaliana. Plant J 58: 499–510

Tamagnone L, Merida A, Stacey N, Plaskitt K, Parr A, Chang CF, Lynn D, Dow JM, Roberts K, Martin C (1998) Inhibition of phenolic acid metabolism results in precocious cell death and altered cell morphology in leaves of transgenic tobacco plants. Plant Cell 10: 1801–1816

Tanksley SD, Ganal MW, Prince JP, de Vicente MC, Bonierbale MW, Broun P, Fulton TM, Giovannoni JJ, Grandillo S, Martin GB, et al (1992) High density molecular linkage maps of the tomato and potato genomes. Genetics 132: 1141–1160

Tronchet M, Ranty B, Marco Y, Roby D (2001) HSR203 antisense suppression in tobacco accelerates development of hypersensitive cell death. Plant J 27: 115–127

Wang L, Tu YC, Lian TW, Hung JT, Yen JH, Wu MJ (2006) Distinctive antioxidant and antiinflammatory effects of flavonols. J Agric Food Chem 54: 9798–9804

Wessinger CA, Rausher MD (2012) Lessons from flower colour evolution on targets of selection. J Exp Bot 63: 5741–5749

Winkel-Shirley B (2001) Flavonoid biosynthesis: a colorful model for genetics, biochemistry, cell biology, and biotechnology. Plant Physiol 126: 485–493

Zhang Y, Butelli E, De Stefano R, Schoonbeek HJ, Magusin A, Pagliarani C, Wellner N, Hill L, Orzaez D, Granell A, et al (2013) Anthocyanins double the shelf life of tomatoes by delaying overripening and reducing susceptibility to gray mold. Curr Biol 23: 1094–1100

Zhang Y, Butelli E, Martin C (2014) Engineering anthocyanin biosynthesis in plants. Curr Opin Plant Biol 19: 81–90

Zidenga T, Leyva-Guerrero E, Moon H, Siritunga D, Sayre R (2012) Extending cassava root shelf life via reduction of reactive oxygen species production. Plant Physiol 159: 1396–1407